AD-A040 426 GRUMMAN AEROSPACE CORP BETHPAGE N Y RESEARCH DEPT F/G 17/8
BASELINE TEST OF A MATCHED FILTER CORRELATOR FOR SCREENING AERI--ETC(U)
MAY 77 K G LEIB, M R WOHLERS, R HEROLD

UNCLASSIFIED RE-540 NL

| OF |
AD A040426

END

DATE FILMED
7-77

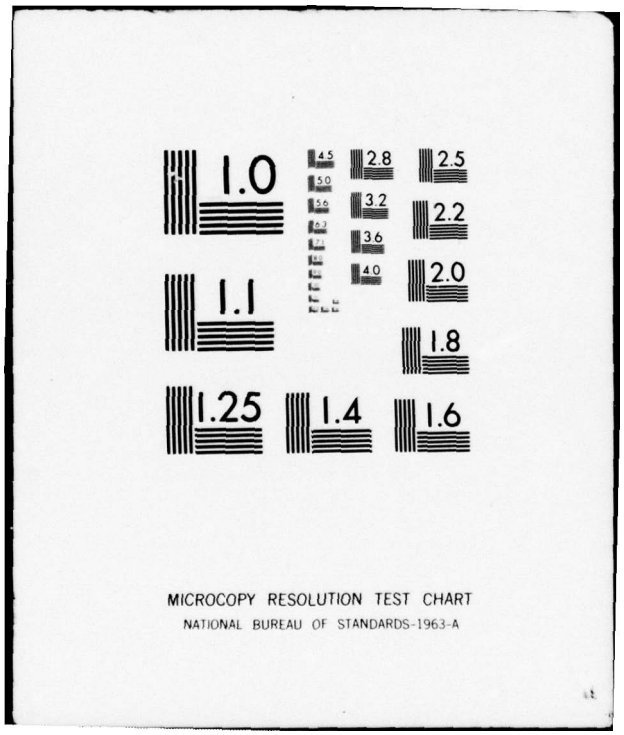
1.0
1.1
1.25
1.4
1.6
1.8
2.0
2.2
2.5
2.8
3.2
3.6
4.0
4.5
5.0
5.6
6.3
7.1
8
9
10
11
12
13
14
16
18
20
22
25
28
32
36
40
45
50
56
63
71
80
90
100
MICROCOPY RESOLUTION TEST CHART
NATIONAL BUREAU OF STANDARDS-1963-A

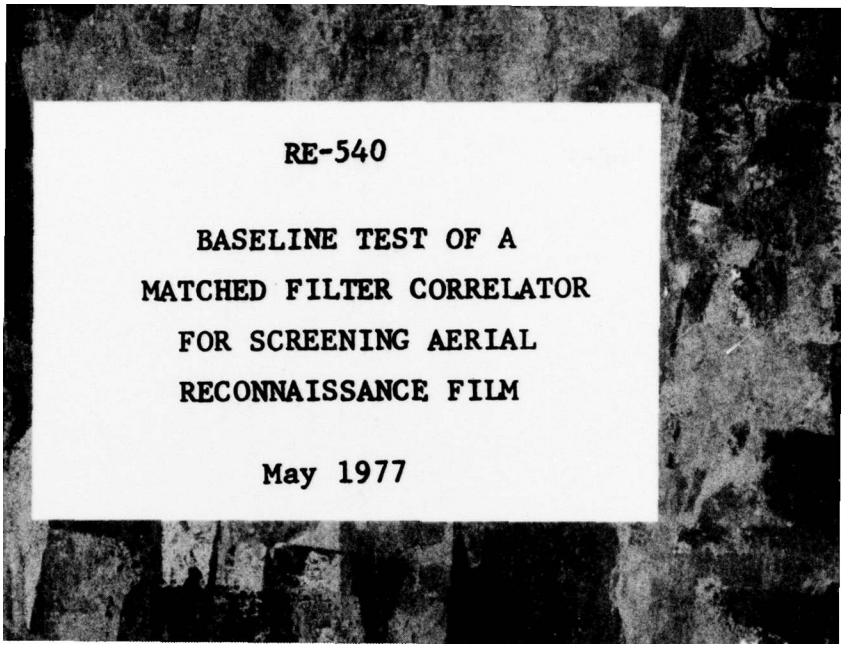

RE-540

BASELINE TEST OF A MATCHED FILTER CORRELATOR FOR SCREENING AERIAL RECONNAISSANCE FILM

May 1977

Unclassified

SECURITY CLASSIFICATION OF THIS PAGE *(When Data Entered)*

REPORT DOCUMENTATION PAGE		READ INSTRUCTIONS BEFORE COMPLETING FORM
1. REPORT NUMBER RE-540	2. GOVT ACCESSION NO.	3. RECIPIENT'S CATALOG NUMBER
4. TITLE *(and Subtitle)* Baseline Test of a Matched Filter Correlator for Screening Aerial Reconnaissance Film		5. TYPE OF REPORT & PERIOD COVERED Report 6. PERFORMING ORG. REPORT NUMBER RE-540
7. AUTHOR(s) Kenneth G. Leib, M. Ronald Wohlers Ronald Herold		8. CONTRACT OR GRANT NUMBER(s) N/A
9. PERFORMING ORGANIZATION NAME AND ADDRESS Grumman Aerospace Corporation Bethpage, New York 11714		10. PROGRAM ELEMENT, PROJECT, TASK AREA & WORK UNIT NUMBERS N/A
11. CONTROLLING OFFICE NAME AND ADDRESS N/A		12. REPORT DATE May 1977 13. NUMBER OF PAGES 66
14. MONITORING AGENCY NAME & ADDRESS*(if different from Controlling Office)* N/A		15. SECURITY CLASS. *(of this report)* Unclassified 15a. DECLASSIFICATION/DOWNGRADING SCHEDULE

16. DISTRIBUTION STATEMENT *(of this Report)*

Approved for Public release; distribution unlimited

17. DISTRIBUTION STATEMENT *(of the abstract entered in Block 20, if different from Report)*

N/A

18. SUPPLEMENTARY NOTES

N/A

19. KEY WORDS *(Continue on reverse side if necessary and identify by block number)*

20. ABSTRACT *(Continue on reverse side if necessary and identify by block number)*

An optical matched filter image correlator previously reported upon was used to perform a screening mission on aerial reconnaissance film with limited sampling of various terrain imagery. The sampling was limited to several scans of each image in the correlator plane. The target was generally recognizable when the signal-to-clutter ratio was in the range of one to ten dB depending upon the type of terrain and the band pass char-

DD FORM 1 JAN 73 1473 EDITION OF 1 NOV 65 IS OBSOLETE
S/N 0102-014-6601 |

Unclassified

SECURITY CLASSIFICATION OF THIS PAGE *(When Data Entered)*

acteristics (or order) of the matched filter used. In some cases false alarm detection was experienced and a tradeoff between false alarms or clutter, and probability of detection can be made.

The results obtained through the sampling of the correlation plane show that the probability of detection could be 99 percent for the most complex terrain encountered if 10.5 percent false alarm rate are also accepted. Thus, the correlator can perform the screening mission. Predictions on the system detection of targets in various terrain are given.

(13)

(14) Grumman Research Department Report RE-540

(6) BASELINE TEST OF A MATCHED FILTER CORRELATOR FOR SCREENING AERIAL RECONNAISSANCE FILM

by

(10) Kenneth G. Leib
M. Ronald Wohlers
Ronald Herold

System Sciences

(11) May 1977

(12) 68 p.

Approved by: Richard A. Scheuing
Richard A. Scheuing
Director of Research

ABSTRACT

An optical matched filter image correlator previously reported upon was used to perform a screening mission on aerial reconnaissance film with limited sampling of various terrain imagery. The sampling was limited to several scans of each image in the correlator plane. The target was generally recognizable when the signal-to-clutter ratio was in the range of one to ten dB depending upon the type of terrain and the band pass characteristics (or order) of the matched filter used. In some cases false alarm detection was experienced and a tradeoff between false alarms or clutter, and probability of detection can be made.

The results obtained through the sampling of the correlation plane show that the probability of detection could be 99 percent for the most complex terrain encountered if 10.5 percent false alarm rate are also accepted. Thus, the correlator can perform the screening mission. Predictions on the system detection of targets in various terrain are given.

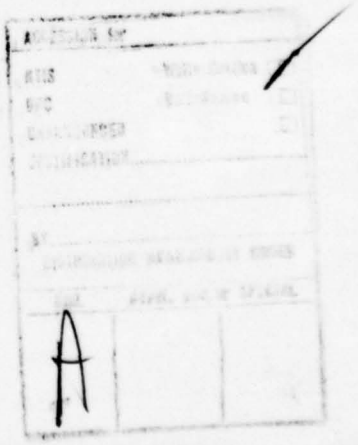

TABLE OF CONTENTS

LIST OF ILLUSTRATIONS

LIST OF TABLES

1. INTRODUCTION

In a previous investigation (Ref. 1) the sensitivity of a matched filter in an optical correlator to variations in several of the object's parameters was studied. The study also presented an examination of the ability to identify the object (an M-60 tank) in a limited number of terrain scenes where the differences were relatively minor. It was clear, however, that the object could be identified within that class of background. In all cases, the imagery for parametric sensitivity, as well as the identification phases of that study, was recorded on film. Other studies (e.g., Ref. 2 and its continuation) are considering similar problems through the use of a real time transducer.

This report is an extension of the work described in Ref. 1 as it applies to a screening operation in an aerial reconnaissance mission. In this case screening means the processing of acquired film so that photointerpreters or field commanders need only survey particular frames of interest. The work is limited in that it represents only a sampling of the information available for processing and therefore is subject to all usual uncertainties inherent in the interpretation of limited data.

Specifically, a set of imagery was prepared in which the presence and disposition of targets was varied, and in which the background was given significant variability. Then the imagery was played through what is referred to as the baseline correlator and several scans made in the correlation plane with a fiber optic probe. The baseline correlator is the OMFIC system described in the next section. Reduction of the data yielded the relative signal levels, signal-to-clutter ratios, false alarms, etc., as required for all of the imagery used in a particular sequence. In

addition, an analysis of the detection performance of a "prototype" OMFIC configuration is given, and some of the data obtained in this program are used to present the results of that analysis.

2. DESCRIPTION OF BASELINE CORRELATOR AND MATCHED FILTERS

The optical matched filter image correlator (Fig. 1) used in this investigation is similar to that reported upon in Ref. 1, with a minor exception. Some parameters of this system are as follows:

Offset Angle	10
Transform Lens	Schneider Tele-Xenar 360/f:5.6
Inverse Transform Lens	Schneider TV-Xenon 100 mm
MF Recording Plates	EK 120-02
Object Film	35 mm SO 173
Spectral Sensitivity	4.39 cycles/mm per mm

The setup is configured so the matched filters can be fabricated directly without altering the system. Prior to matched filter fabrication, the spectrum of the tank was scanned with a 450 μm probe, the result of which is shown in Fig. 2. Each of the peaks away from the center are the lobes, or orders of the spectrum and refer to the various spatial frequency bands of the spectrum. The matched filters are made by maximizing the fringe visibility of the particular order or lobe, and thus form the third, fourth, etc., order matched filter. The peak intensity of a particular order forms the basis for establishing appropriate R = (Reference Beam Intensity/Signal Beam Intensity) ratios used in making the filters. As it turned out, the values for the first

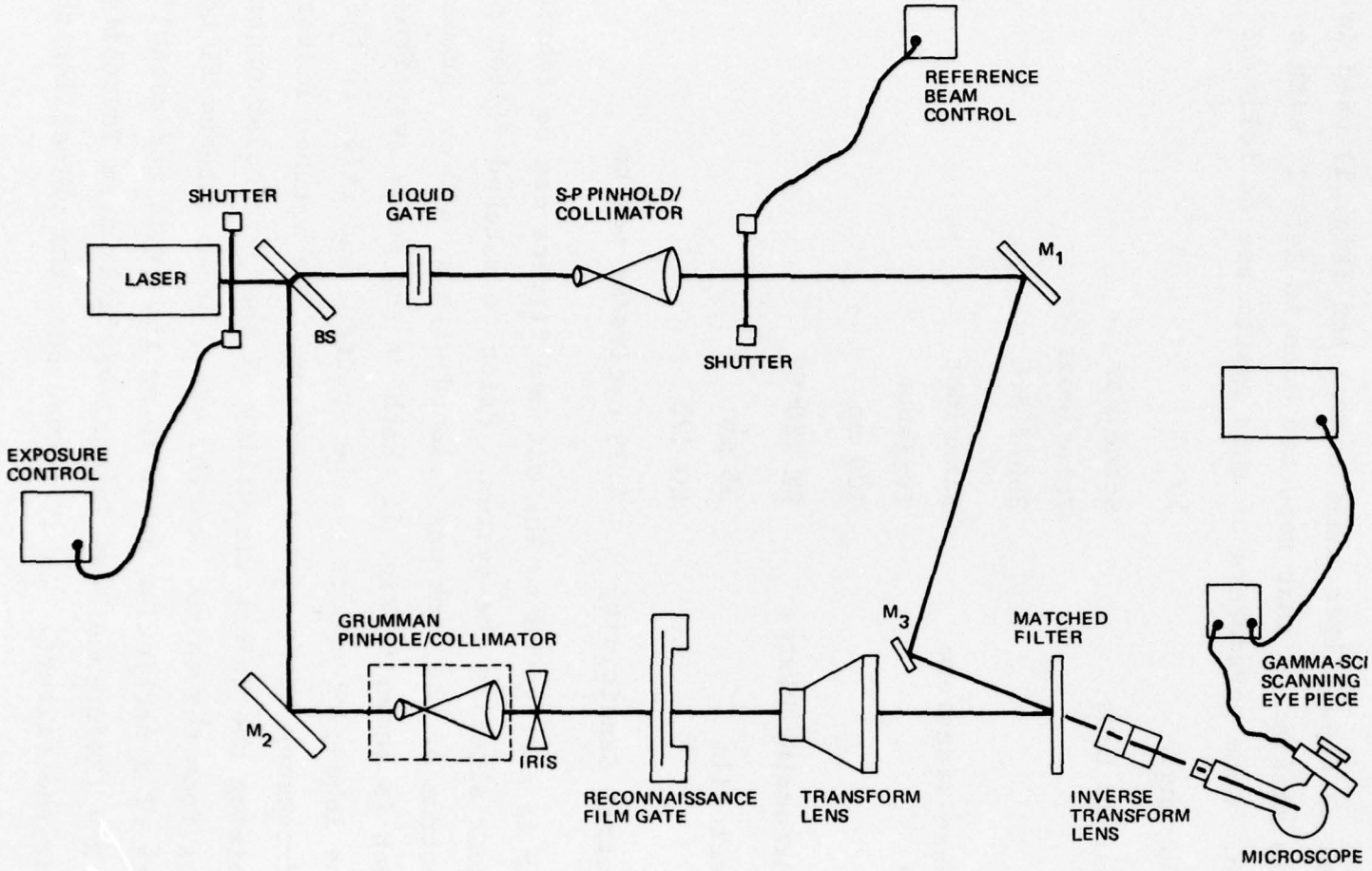

Fig. 1 Experimental Arrangement for Matched Filter Fabrication and Correlation Measurements

three orders (or lobes) were relatively equal (see Fig. 2) so that a single beam intensity ratio enabled the first three orders to be recorded in one exposure. For each order, bracketing exposures were made to yield a range of amplitude transmittance values for each order matched filter that was fabricated.

The primary target of interest was the same as in the previous study (Ref. 1), namely, the M-60 A1 U.S. Army tank shown in Fig. 3. Its spectrum was scanned along an axis perpendicular to the major tank axis and is shown in Fig. 2. In the present study, the tank used for matched filter preparation was a 0.97 x 1.94 mm, 40 cycle per mm computer generated image. The terrain imagery described in Section 3 was analog generated (directly filmed) although the tank model included in the imagery was also used to form the image which was used in digitizing.

Since this image was smaller than that used in Ref. 1, the location of the different Fourier spectrum lobes (squared) is $(0.97)^{-1}$ further out than those given in that reference. The new spatial frequencies are given in Table 1 and as in that case, are based upon an equivalent rectangle.

In the same setup upon playback, the peak autocorrelation value was measured for each filter. The optimum filter for each order was then considered to be the one with the peak autocorrelation value. The result of this matched filter evaluation is summarized in Fig. 4 which shows the relative correlation, $\hat{C}$, for each filter in the exposure bracket for each order. Note that for the sixth order, an apparent correlation peak was not reached. From experience, use of the last sixth order filter as the optimum is considered a more likely choice than using one selected from a new set of bracketed exposures using a different emulsion batch, ... a prospect to be faced at the time additional filters were to be made.

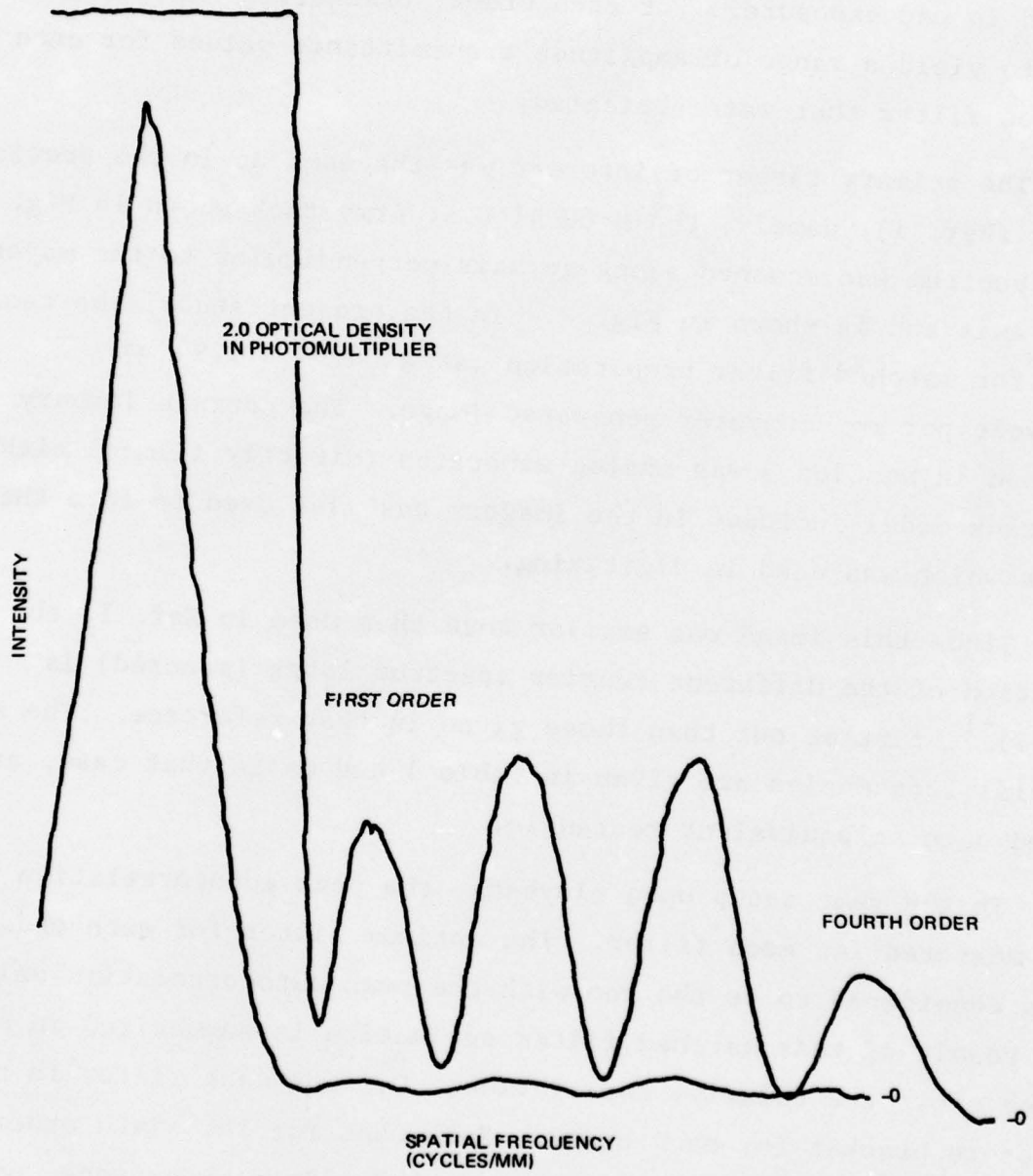

Fig. 2 M-60 Spectrum Scan Perpendicular to Major Axis (Parameters: 450 μm Probe; 4.39 $\frac{\text{cycles}}{\text{mm}}$ /mm Scale Sensitivity; 360mm Focal Length)

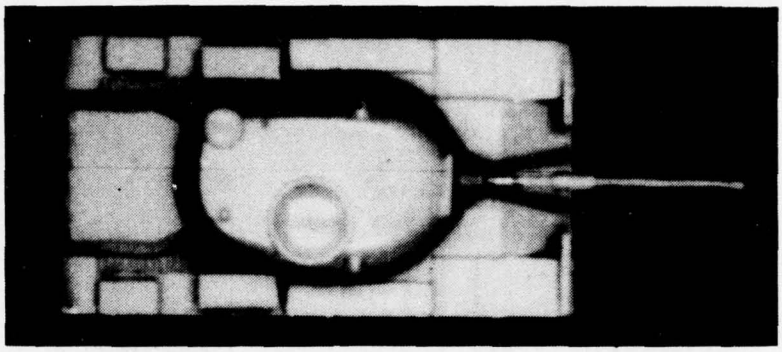

Fig. 3 M-60 Tank Image (Actual Size 0.97mm x 1.94mm)

TABLE 1 LOCATION AND SPATIAL FREQUENCY OF M-60 MATCHED FILTER ORDERS

Relative Position	Location	Spatial Frequency
DC (or Zero Order Peak	centerline	0 cycles/mm
First Null	0.225 mm	0.99
First Order Peak	0.322	1.47
Second Null	0.450	1.97
Second Order Peak	0.553	2.42
Third Null	0.676	2.96
Third Order Peak	0.782	3.43
Fourth Null	0.900	3.95
Fourth Order Peak	1.009	4.42
Fifth Null	1.123	4.99
Fifth Order Peak	1.227	5.39
Sixth Null	1.351	5.91

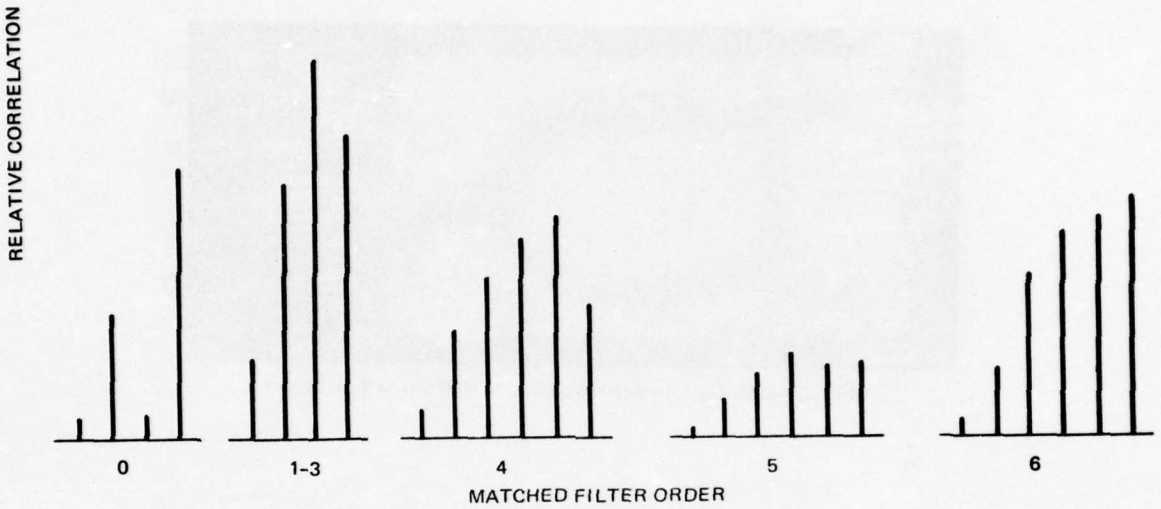

Fig. 4 Comparison Between Matched Filters Showing Distribution Within Bracket For Each Order

Two of the elements in Fig. 1 might require some additional explanation. The reconnaissance film gate is a decahydroethylene filled liquid gate capable of enabling up to 100 feet of 35 mm film to be transported and registered according to a preset indexing.

The correlation planes were scanned with a fiber optic probe, scanning eyepiece mounted on a microscope fitted with a 5x objective lens. In most cases, the probe was 50 μm in diameter although as previously indicated, the spectrum was scanned with a 450 μm probe. In addition, a few tests were conducted with the latter. No intermediate choices were available.

3. CHARACTERISTICS OF THE RECONNAISSANCE FILM IMAGERY

The reconnaissance film imagery used in this investigation consisted of eight different background terrains, three of which contained targets of interest. The imagery was originally obtained by photographing various portions of a 400/1 scaled simulation model located at the Night Vision Laboratory at Fort Belvoir. The original 4 x 5 in. negatives were obtained through the courtesy of the U.S Army.

Since positives are used in the baseline system, the negatives were photographed to form a sequence of 22 frames on a 35 mm film strip. This strip was then mounted in the Grumman liquid gate and played through the system. The scale of the imagery was 1:3800.

The scenes are described below in the same sequence as they appear on the film strip and are shown in Figs. 5 through 8, respectively. Note that only a circular portion generally centered about the M-60 tank (when present) was the portion optically processed. The size of this aperture is shown in Fig. 9 to the same relative scale as the terrain images shown in Figs. 5 through 8. Reference to the summary in Table 2 should also be made during the review of the scenes.

SCENE 1 (Woodland, Fig. 5a)

The actual frame used in this program is similar to the one shown in Fig. 6a. However, it included only the M-60 tank as shown, without the other targets. Only one such frame of this type was available in the test strip. About 80 percent of the processed scene was tree covered. In most cases, the autocorrelation signal in this scene formed the reference signal for establishing signal-to-clutter ratios.

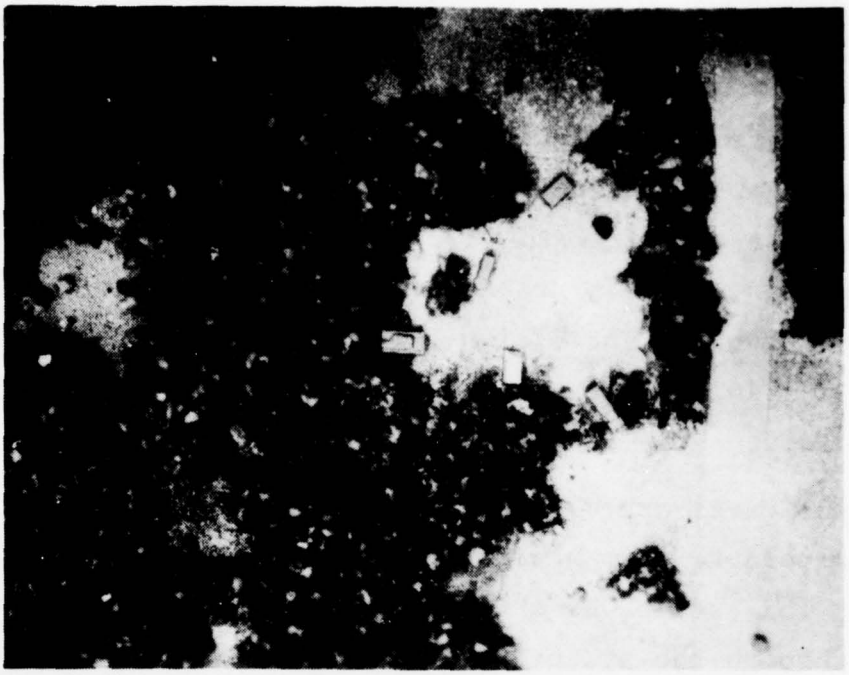

(a) WOODLAND

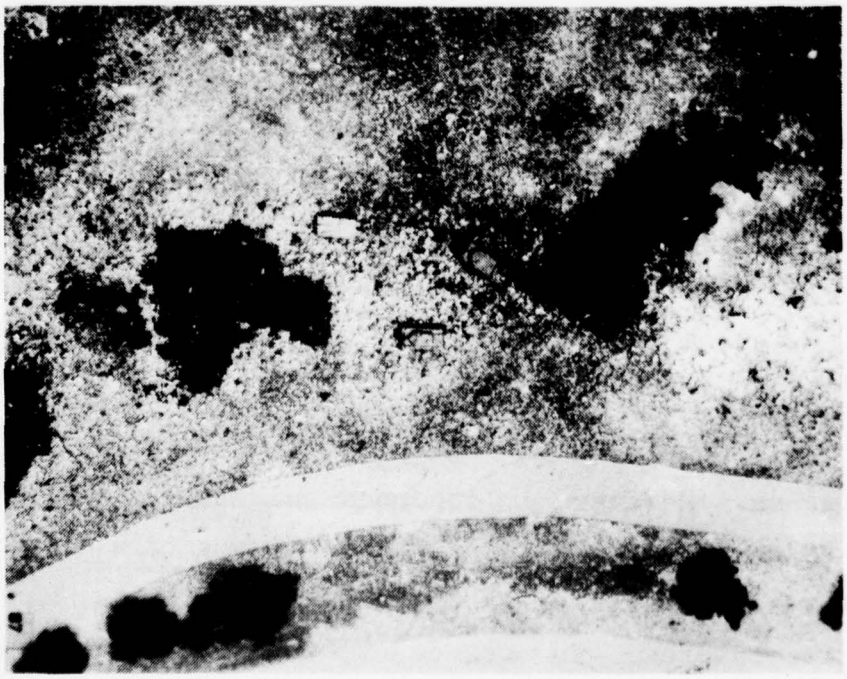

(b) ROADSIDE

Fig. 5 Woodland (a) and Roadside (b) Terrain Scenes

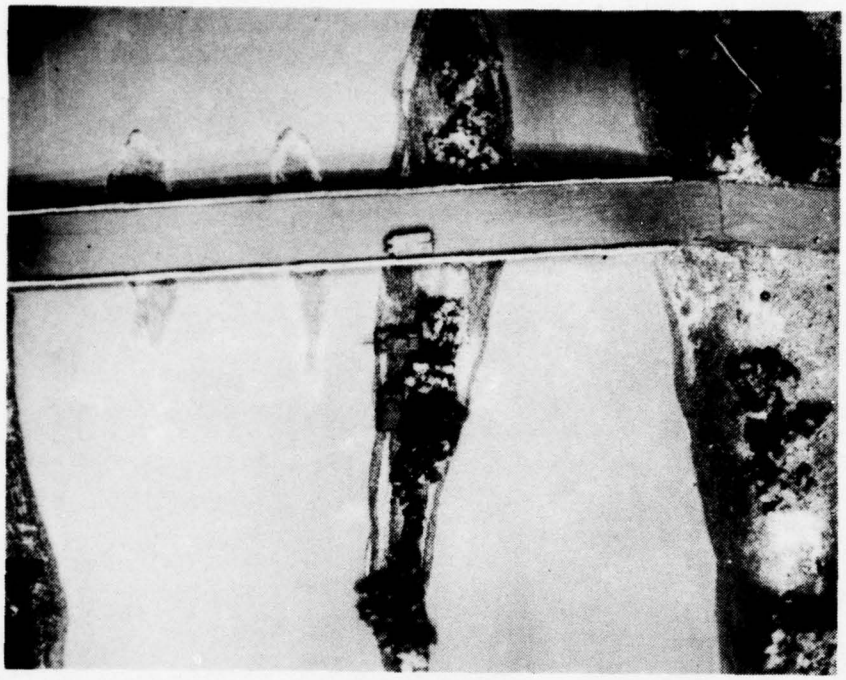

(a) RIVER/ISLAND

(b) TOWN CIRCLE

Fig. 6 River/Island (a) and Town Circle (b) Terrain Scenes

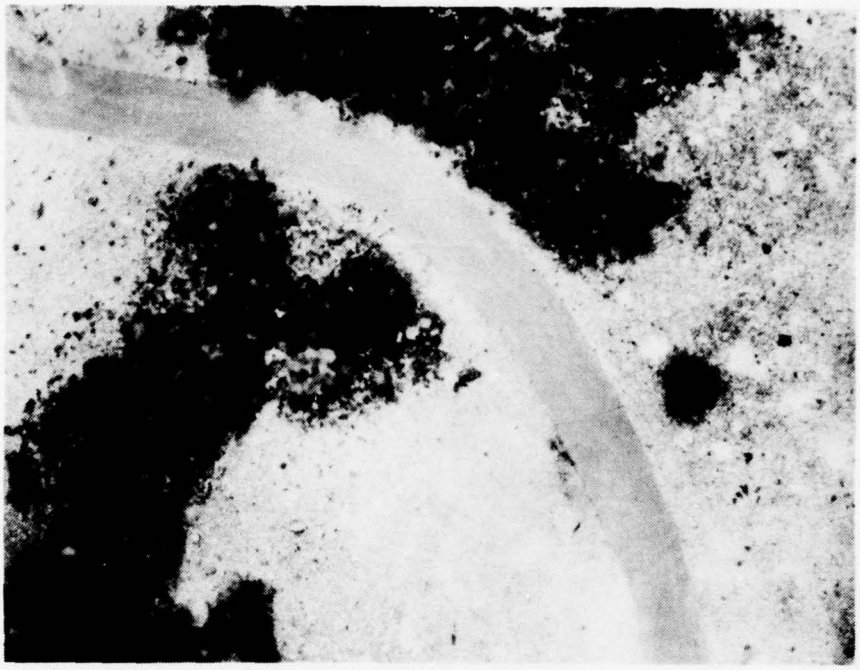

(a) CURVED ROAD

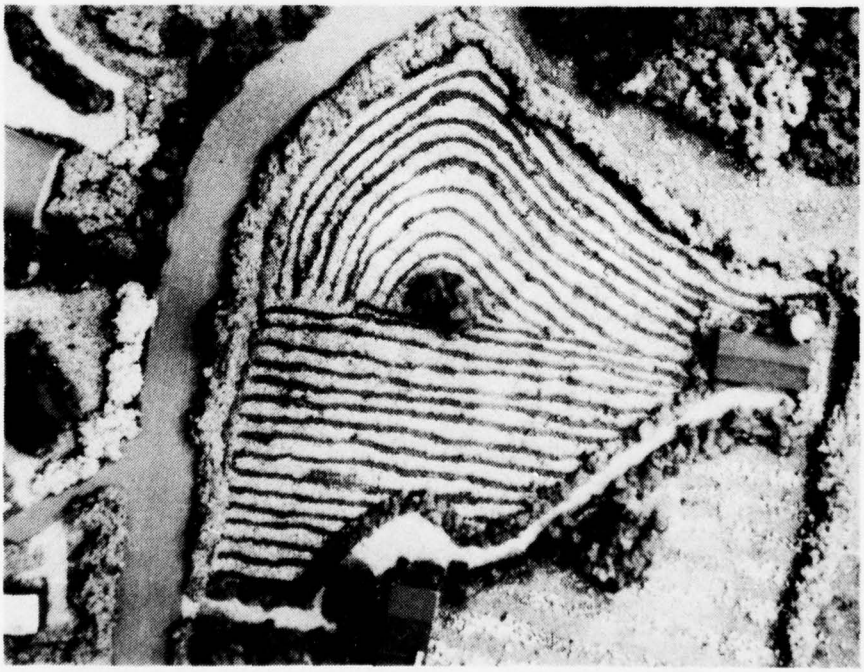

(b) FARMLAND

Fig. 7 Curved Road (a) and Farmland (b) Terrain Scenes

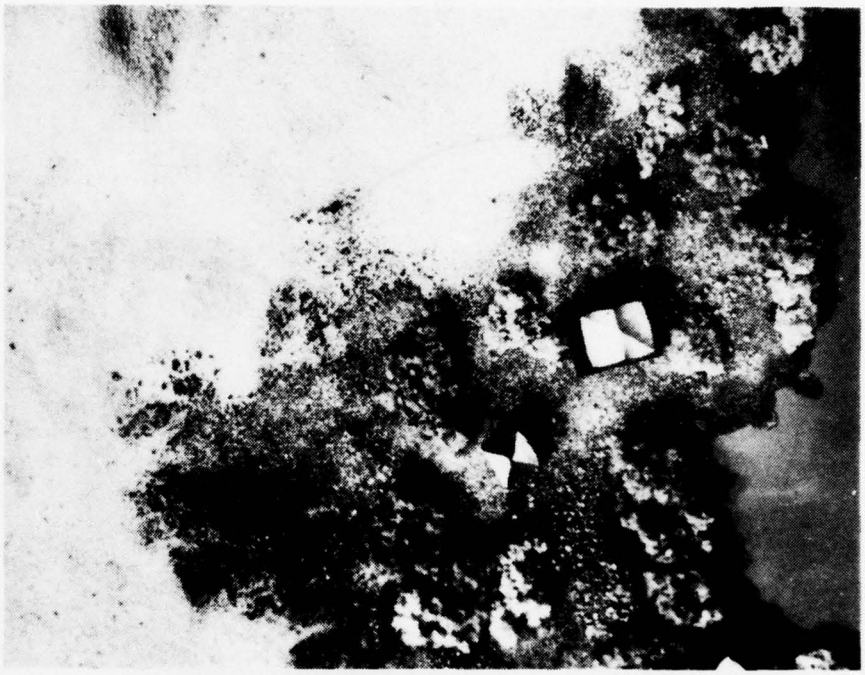

(a) MID-EAST

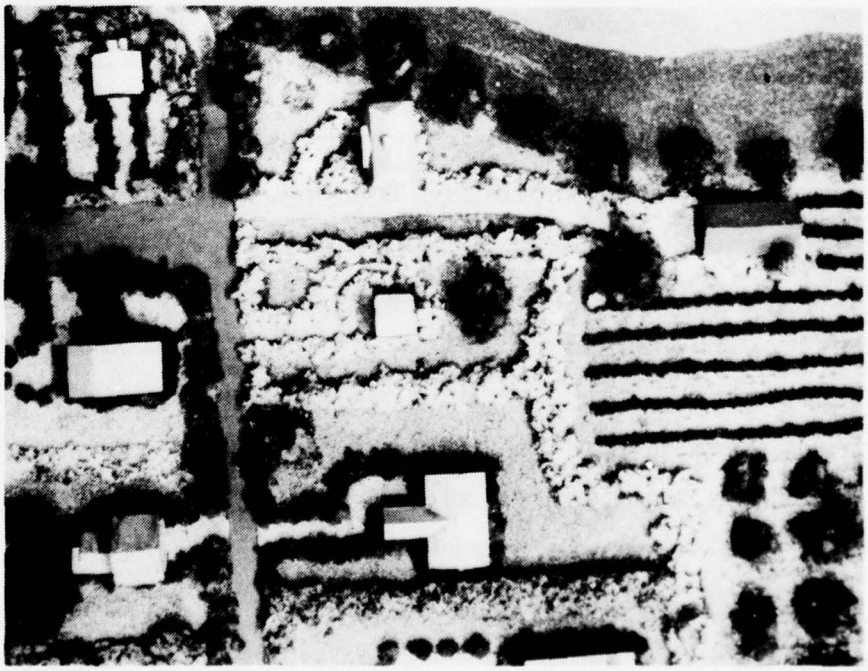

(b) VILLAGE

Fig. 8 Mid-East (a) and Village (b) Terrain Scenes

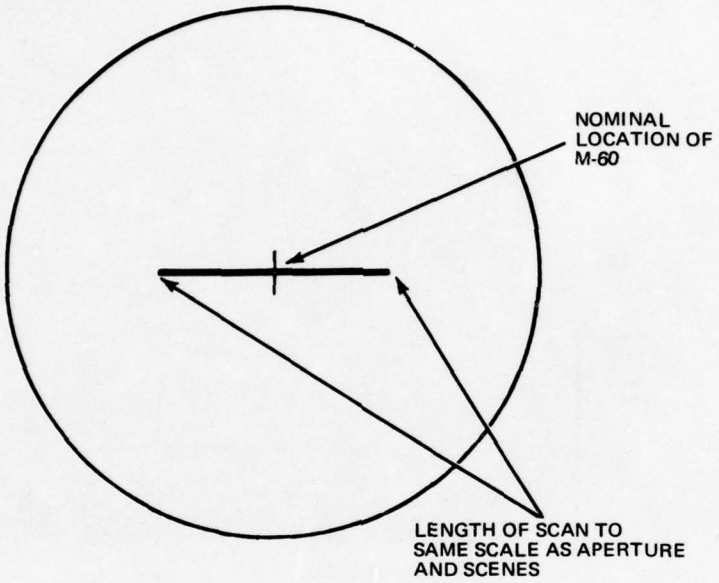

Fig. 9 Nominal Aperture Size Shown To Same Scale as Terrain Scenes

SCENE 2 (Roadside, Fig. 6b)

There were eight frames with this relatively open scene with the variations shown in Table 2. The one illustrated was No. 2b and contained the three tanks: M-60, Soviet T-62, and Swedish "S" tank. When the T-62 frames were taken, the T-62 replaced the M-60 at the center although in practice, slight differences in actual position resulted. Scenes 2c and 2d are identical with the latter being a low contrast version of the former, and were generally not included in the sequential data except as noted. About 95 percent of the processed scene was open country.

TABLE 2 BASELINE 35 mm FILMSTRIP

Terrain Scene Number	Description	Transmission %	Average Optical Density	Targets Present
1	Woodland	25.0	0.60	M-60
2a	Roadside	43.4	0.36	M-60
2b	"	44.4	0.35	M-60, T-62, S
2c	"	41.5	0.38	M-60 + 5 Targets†
2d	"	75.6	0.12	Same; Low Contrast
2e	"	42.2	0.38	T-62 + 5 Targets
2f	"	41.5	0.38	T-62
2g	"	42.7	0.37	5 Targets
2h	"	43.2	0.37	None
3a	River/Island	61.9	0.21	M-60
3b	"	61.9	0.21	B/W M-60's
3c	"	65.3	0.19	M-60, T-62, S
3d	"	61.4	0.21	M-60 + 5 Targets
3e	"	60.2	0.22	T-62
3f	"	65.3	0.19	T-62 % Targets
3g	"	63.1	0.20	5 Targets
3h	"	59.7	0.22	None
4	Town Circle	58.5	0.23	None
5	Curved Road	62.5	0.20	None
6	Farmland	45.6	0.34	None
7	Mid East	47.7	0.32	None
8	Village	50.6	0.30	None

†5 Targets: 3 different trucks + 2 different APC's

SCENE 3 (River/Island, Fig. 6a)

There were eight variations of this scene in the test film strip. The same conditions generally prevail regarding the T-62/M-60 interchange. The illustration given represents Scene 3c (Table 2). In Scene 3b, there were two M-60 tanks along the roadway in positions on either side of the APC shown. These tanks were black and white versions of the same OD tank otherwise used in the scenes.

SCENE 4 (Town Circle, Fig. 6b)

The processed scene was centered approximately around the circle and therefore included portions or all of three houses shown nearest the center. In this and all subsequent scenes, no targets are present.

SCENE 5 (Curved Road, Fig. 7a)

This is a relatively open scene without targets and is similar to the roadside scene. The processed portion had approximately 25 percent tree covering.

SCENE 6 (Farmland, Fig. 7b)

The major portion of the processed scene was the central arrangement of periodic rows. Examination shows that many portions of the row period are close to the width of the tank.

SCENE 7 (Mid East, Fig. 8a)

This is a scene with approximately equal portions of sandy soil and low ground cover. Two tents are included in the processed scene.

SCENE 8 (Village, Fig. 8b)

This scene has a wide variation in contrast and construction, and has three buildings of different sizes as well as discrete tree clumps.

The transmission of each of these scenes is given in Table 2 along with the corresponding average optical density. These were measured with a 19 mm aperture. The film strip was processed with a 24 mm apodized aperture so that the transmissions and densities are representative only. Also, in processing various sequences it cannot be assumed that each scene was precisely in the same position for each sequence. This uncertainty arises from the nature of the wind/rewind mechanism of the film transport gate.

As indicated previously, the imagery was played through the system containing a 24 mm apodized aperture whose falloff was approximately Gaussian over the outer one millimeter radius. This aperture was necessary because of the extraneous signals that would be introduced into the correlation plane by a sharp aperture, even when the (Area of target/Area of aperture) ratio is large. The need for this approach is discussed in Ref. 1.

In general, the results presented below were obtained as a result of three, four, or five horizontal scans according to the particular sequences. Each of the scans was one centimeter in length in the correlation plane. The first scan was always through the target, or target position, and the others were at the nominal extremes and midpoints in the field of view at the correlation plane. Figure 9 shows the approximate positions of the scans related back in size to the input plane. For sequences like the "worst case" scans, obviously this pattern could not be used.

It is of interest to note that with the optics employed in the investigation the 50 μm probe corresponds to a scan in the object plane of approximately one half of a standard television line.

4. RESULTS OF BASELINE TESTS

The purpose of this investigation was to determine whether the matched filter correlator could perform an aerial reconnaissance film screening operation. If, in this investigation, a sampling of the information available in the correlator gave a sufficient indication of its use in this role, then a full scale, full correlation plane assessment would be warranted.

The results of this investigation were obtained from a series of tests that usually had a single objective within that test set. In this way, it was thought that relationships arising would at least be valid and consistent within that test set. It was believed that this approach would also effectively increase the sampling of the information available by requiring a multiplicity of data scans for a given film. This approach lends itself to some inconsistencies in the data because a correlation plane scan is not precisely repeatable. However, the virtues of the approach adapted are considered to outweigh the development of all relationships from a single set of data.

Note also that scans through peak values, such as autocorrelation peaks, could not always be assured on each run. Fortunately this error of omission, when it occurred, was on the conservative side.

Within all of these limitations then, the results of the sequence are reported upon below.

SIGNAL-TO-CLUTTER (S/C) RATIO AND FALSE TARGET THRESHOLD LEVELS IN SELECTED SEQUENCES

The sequence of photographs numbered 1, 4, 5, 6, 7, and 8 were optically processed through a third order matched filter optimized

on the autocorrelation signal in the woodland scene, No. 1. This was the only scene with a target. Five scans were used for each scene. The purpose of this test was to sample the S/C ratio for all nontarget scenes normalized against a single target containing a woodland scene.

The autocorrelation peak of the woodland scene was used as the reference signal by selecting the peak as the zero dB threshold level. Then, the -3 dB and -6 dB levels were determined from the reference signal. For each of the three threshold levels, the number of peak signals (one real, the others false targets) exceeding the three thresholds were counted for each scene. These results are shown in Table 3.

In addition, the signal-to-peak clutter present in any of the five scans was also measured for each scene. It is given in the second column but in terms of the level at which it would be sensed; thus, the S/C ratio would be the positive value of

$$\frac{\text{Signal}}{\text{Clutter}} = \frac{\text{Autocorrelation peak, } \hat{C} \text{ in No. 1}}{\text{Peak clutter in given scene}}$$

It can be seen that the first false target is reached at the -3 dB threshold level but that many false targets are indicated at the -6 dB level. The true target is, of course, present at all levels, and the only signal until a threshold of -2.5 dB is passed. It should be noted that both scenes in which furrows whose spacing is approximately the width of the tank, have the largest number of false alarms. The last scene also contains a structure in the center, whose dimensions are close to the tank length.

TABLE 3 TARGET DETECTION AS FUNCTION OF THRESHOLD LEVEL (THIRD ORDER MATCHED FILTER)

	Level of First False	$\hat{C}$ = 0 dB	-3 dB	-6 dB
Woodland	-6.52	1	1	1
Town Circle	-4.32	0	0	7
Curved Road	-4.60	0	0	5
Farmland	-2.53	0	1	8
Mid East	-5.19	0	0	2
Village	-3.31	0	0	9
	Totals:	1 (Real)	2	32

SIGNAL-TO-CLUTTER AND RELATIVE SIGNAL STRENGTH IN TARGET CONTAINING SCENES

The woodland scene was again used this time in conjunction with the two other scenes containing M-60 tanks, in order to compare the S/C ratio for all three. These results are shown in Table 4 with the three scans shown in Fig. 10.

TABLE 4 S/C RATIO FOR M-60 IN THREE TERRAIN MODELS USING THIRD ORDER MATCHED FILTER

	Relative Target Signal	S/C Ratio Referred to	
		Maximum Autocorrelation	Minimum Autocorrelation
Woodland	1.00	8.26 dB	5.74 dB
Roadside	0.58	4.95	4.95
River/Island	0.81	3.50	2.10

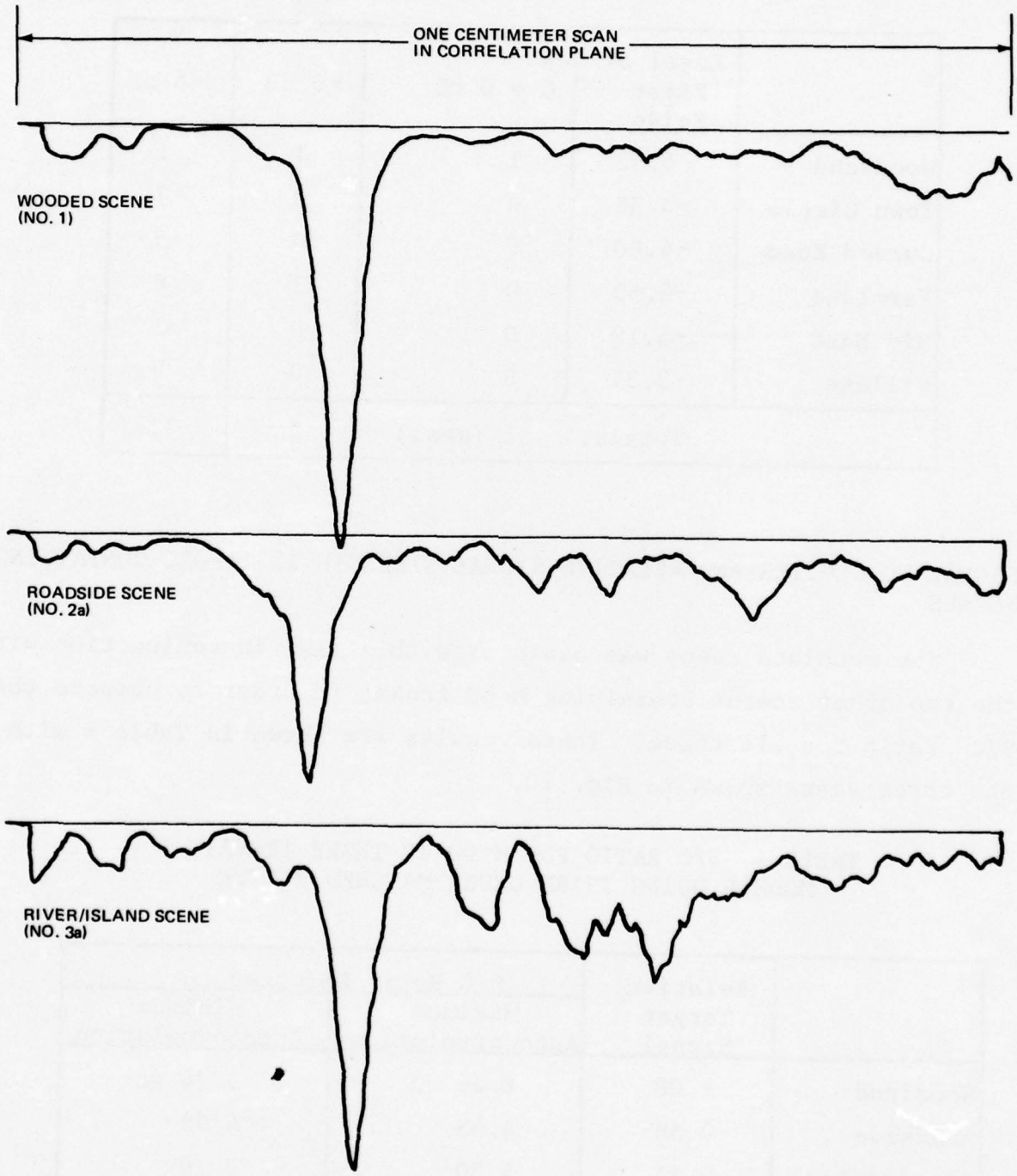

Fig. 10 Single Scans for Scenes Containing M-60 Along Major Tank Axis

Note that the two scenes which have a similar nature — the roadside and curved road scenes — also have similar results when referred to the woodland scene autocorrelation. Likewise, there is some similarity between the "busy" river/island and the farmland or village scenes. While the river/island scene does not have any of the obvious tank length or width periodicities that the other two scenes show, it does have two sets of sharp edges along the road which are parallel to the tank axis, the matched filter orientation.

The data from this test was altered in such a way that the minimum autocorrelation signal (from the roadside scene) was used to establish the S/C ratio. These results are given in the last column of Table 4 where it can be seen that there is still a significant S/C ratio although the river/island scene is below 3 dB. This is surprising in that the visual images of the M-60 tank on these two films appear very similar. On the other hand, the apparent "randomness" of the woodland and roadside scenes gives them a noise character for which the Van der Lugt matched filter is supposed to be optimum.

SIGNAL-TO-CLUTTER COMPARISONS FOR ENTIRE TEST FILM STRIP

The fourth order matched filter was used in a test sequence in which all of the terrain imagery was played through the correlator, and the five scans made in the correlation plane. In this sequence, it was possible to obtain under constant conditions, a relative assessment of the entire film strip.

The data are summarized in Table 5 where the T-62 "other target" data were also identified in frames where it replaced the M-60. The peak clutter, when associated with a T-62 frame, represents the next peak other than the identified T-62. Also, the first S/C column

TABLE 5 S/C RATIO AND RELATIVE SIGNAL LEVEL FOR FOURTH ORDER MF USING BASELINE TERRAIN SCENES

Terrain	Relative Signal			M-60 S/C Ratio	Individual Frame S/C Ratio
	M-60	Other Target	Peak Clutter		
Wooded	1.00	-	0.13	8.86 dB	8.86
Roadside	0.45	-	0.18	7.45	3.98
Roadside	0.45	-	0.18	7.45	3.98
Roadside	0.47	-	0.22	6.58	3.30
Roadside	-	0.28	0.09	5.53	-
Roadside	-	0.34	0.12	4.69	-
Roadside	-	0.20	0.17	6.99	-
Roadside	-	-	0.13	8.86	-
River/Island	0.44	-	0.23	6.38	2.82
River/Island	0.48	-	0.18	7.45	4.26
River/Island	0.68	-	0.32	4.95	3.27
River/Island	0.60	-	0.31	5.09	2.87
River/Island	-	0.24	0.33	4.81	-
River/Island	-	0.45	0.31	3.47	-
River/Island	-	0.15	0.18	7.45	-
River/Island	-	-	0.21	6.78	-
Town Circle	-	-	0.21	6.78	-
Curved Road	-	-	0.14	8.54	-
Farmland	-	-	0.17	7.70	-
Mid East	-	-	0.20	6.99	-
Village	-	-	0.21	6.78	-

represents the S/C ratio using the woodland scene autocorrelation peak as reference while the second S/C column is computed only for that frame.

Several interesting results appear to emerge from the data. First, there seems to be an over-all higher level of discrimination with the fourth order filter (more on this is discussed later). A comparison of the information in Table 3 with the results for the first and last five scenes makes this apparent. There does not seem to be any highest-lowest correspondence. However, considering that the scenes have different Fourier transforms suggests once again that the best matched filter selected on the basis of largest autocorrelation is not necessarily the best filter for discriminating between targets under all terrain conditions.

It is not clear why the relative signal for the tanks in the river/island scene are as wide apart as they are. Observation of the images does not reveal any discernible differences in the appearance of the tank. Also, the scenes were photographed at the same time. Thus, the conclusion is that as happened often during the scans, the peak of the M-60 autocorrelation was not always the scanned value.

It can be seen that there is always a condition where S/C is less than 1.0 and the maximum clutter in any scene was always less than the minimum signal. The exception is the magnitude of the other target signal, the T-62; the latter is generally less than the M-60 signal. Furthermore, it is not clear why the minimum M-60 autocorrelation peak is about the same as the maximum T-62 in the river/island scene. The experience throughout this investigation has shown the river/island autocorrelation peak to fall between the woodland and roadside peaks with the latter being the lowest. While

the data are presented as obtained, it is suggested that this represents a true anomaly (along with its neighbor). The same cannot be said for the roadside values of the autocorrelation which indicate consistency and a relatively constant value over many scans (but not all reported upon).

Over-all then, these results show a relatively good level of discrimination. Because they were obtained in one continuous processing sequence, the comparisons within the data set have not been influenced by outside conditions and as such are considered acceptable, except as noted.

The scan plots from this sequence with the fourth order filter were analyzed by establishing a threshold using the minimum autocorrelation signal, and then determining the number of real or false targets exceeding this value. Then, one half of this value was taken for the threshold and the process repeated. The results are shown in Table 6. The number of scan lines is based upon five lines per frame. It should be noted that the centerline scan for one of the river/island scenes (Fig. 3b) was through the tank on the bridge, not through a tank at the usual location on the island. The targets detected are separated between real and false, according to the scene. It can be seen that the river/island scene presents many false alarms at the -3 dB level.

"WORST CASE" CLUTTER COMPARISON

Two frames were made available that were neither part of the test sequence nor the contrast set. These were frames comparable to No. 1, woodland, and No. 8, village. The former was exact (Fig. 5a) except for minor density variation while the latter was exact except for the addition of an M-60 tank pointing left and

TABLE 6 DISTRIBUTION OF DETECTED TARGETS USING FOURTH ORDER MATCHED FILTER

Terrain Number	Description	Number of Scan Lines	Targets Detected			
			Real		False	
			Threshold	-3 dB	Threshold	-3 dB
1	Woodland	5	1	1	0	0
2	Roadside	35	3	3	0	2
3	River/Island	40	4	4	1	36
4	Town Circle	5	0	0	0	0
5	Curved Road	5	0	0	0	0
6	Farmland	5	0	0	0	1
7	Mid East	5	0	0	0	3
8	Village	5	0	0	0	2

located between the two hedges just below the center house (Fig. 8b). For this scan, the light distribution aperture was a nonapodized, 18 mm aperture approximately centered about the tank. This was necessitated because the 35 mm image strip had to be rotated 180 degrees to correctly orient the frame with respect to the matched filter. In this case scans were made specifically to include the maximum clutter ostensibly contributed by the houses in the upper and lower portions of the frame. The inclusion of aperture induced clutter should be considered a contributing factor, although attempts to identify this contribution were made.

Three sequences were conducted. In the first, the woodland scene was used to establish a signal reference and the nontarget scenes scanned for the visually perceived worst clutter. This was performed using the film strip. Then, using the two individual

frames referred to above, the correlation planes were scanned for worst noise using four different order matched filters. Finally, the two frames were examined again using the third order filter and the individual and woodland referenced S/C ratios determined. The woodland and village scenes are compared here (and, for example, in Table 3). The former represents the terrain closest to a stationary one while the latter scene represents a complex one with considerable terrain variation.

The results of the first sequence are shown in Table 7 in which the autocorrelation signal in the woodland scene was the reference signal. The results clearly show that the filters respond very differently to different clutter, and that the response of the same clutter to different filters is different. This is further emphasized in the second sequence in which four different order matched filters were used on the woodland and village scenes. This is shown in Table 8 but it must be remembered that the sequences were conducted with two different sets of films (although very close to each other in characteristics) and there were two different apertures used. The latter is important because one of the large clutter areas is the house which falls near the edge of the frame in the 19 mm case.

TABLE 7 S/C RATIO FOR "WORST CASE" SCANS FOR THIRD AND FOURTH ORDER MATCHED FILTER

Scene	S/C Ratio	
	Third Order MF	Fourth Order MF
Town Circle	5.79	5.39
Curved Road	3.88	0.49
Farmland	0.03	(-1.47)
Mid East	3.26	1.46
Village	2.66	2.63

TABLE 8 S/C RATIO ON "WORST CASE" BASIS FOR DIFFERENT ORDER MATCHED FILTERS

	Matched Filter Order			
	1-3	4	5	6
Woodland*	3.31 dB	6.29 dB	6.01	2.12
Village	1.42	2.76	1.95	(-3.18)

*M-60 Autocorrelation signal is reference.

The final sequence consisted of the two individual frames correlated with a third order matched filter. The data are summarized in Table 9 where the woodland scene autocorrelation signal formed the normalizing signal. Then, each frame was individually examined and the S/C ratio formed. The latter is of less importance except if the autocorrelation signal of that frame were the chosen threshold reference.

TABLE 9 S/C RATIO FOR "WORST CASE" CLUTTER USING THIRD ORDER MATCHED FILTER

	Relative Signal		S/C Ratio Normalization	
	Signal	Clutter	Woodland	Frame
Woodland	1.00	0.29	5.39	5.39
Village	0.46	0.58	2.34	-1.05

In these comparisons, it can be seen that the S/C ratio is positive for all but the individual village scene where the clutter is greater. For these scenes, the degree to which the clutter is present is summarized as follows:

	% of Time Clutter Exceeds Threshold† Set at:						
	$\hat{C}$	-1 dB	-2 dB	-3 dB	-4 dB	-5 dB	-6 dB
Woodland Scene	0	0	0	0	0	0	0.71%
Village Scene	0‡	0	0	0.44	1.17	4.13	6.33%

†$\hat{C}$ threshold is M-60 autocorrelation peak in woodland scene.

‡Autocorrelation peak in this scene is -3.0 dB below $\hat{C}$.

The curves from this sequence were examined in some detail by assessing the degree to which a false target is present. This is done by examining the total time false target clutter exceeds a prescribed threshold. For this sequence, the autocorrelation signal C in the woodland scene was measured and established as the zero threshold level. Then, decreasing threshold levels, through 6 dB, were established (with one dB increments) and the false target clutter measured for that threshold value. The duration was then divided by the total sampling time and the percentage false alarm presence computed

$$\% \text{ False Target Presence} = \frac{\sum_{i=0}^{p} (\Delta t)_i}{\sum (t_{scan})} \times 100$$

These results are shown in Table 10 for two critical scenes (one stationary, one cluttered) where different order matched filters are used.

TABLE 10 FALSE TARGET PRESENCE AS A FUNCTION OF THRESHOLD LEVEL FOR DIFFERENT MATCHED FILTERS

Scene	Threshold	Matched Filter Order			
		1-3	4	5	6
Woodland	$\hat{C}$	0.0 %	0.0 %	0.0 %	0.0 %
	-1 dB	0.0	0.0	0.0	0.0
	-2	0.0	0.0	0.0	0.0
	-3	0.0	0.0	0.0	0.64
	-4	0.45	0.0	0.0	2.69
	-5	0.71	0.0	0.0	4.51
	-6	0.9	0.0	0.13	7.71
Village	$\hat{C}$	0.0 %	0.0 %	0.0 %	4.45%
	-1 dB	0.0	0.0	0.0	6.13
	-2	0.38	0.0	0.13	13.01
	-3	1.08	0.17	1.12	16.90
	-4	2.31	0.38	4.12	23.40
	-5	3.08	1.50	7.54	27.37
	-6	7.54	2.21	8.62	34.13

ANALYSIS OF THE DETECTION PERFORMANCE OF A PROTOTYPE OMFIC CONFIGURATION

The intent of this section is to develop an analysis that will utilize the experimental data described previously, and to characterize the performance of an optical matched filter in the presence of various clutter backgrounds. The data described in this report was intended to be representative of the probability of false alarms occurring in the case where the system is designed to look for an M-60 tank. In particular, Table 10 shows the variation of the percentage of false alarms as the threshold or detection level in the correlation

plane is adjusted. It is clear that as the threshold level is reduced, the percentage of false alarms increases. What is not clear is the effect of threshold variations on the target detection performance. If the M-60 target presented to the matched filter was always at the proper scale, orientation, sun illumination condition, etc., then the matched filter would achieve the same target detection performance at any threshold setting below zero dB. However, any or all of the target variables will cause reductions in the output correlation signal as we deviate from the nominal value. The approach taken in this section is to model the variation of target detection with a group of target variables, use this model to compute the variation of target detection probability with a prescribed threshold setting, and finally to merge this analysis with some typical experimental data on clutter or false alarm probability. The net output of the analysis will be a "tradeoff" curve between the percent false alarms or clutter and the percent missed target.

We will model the target detection performance of the matched filter in the presence of changes in target parameters in the simplest possible way. Thus, we will assume that the dependence of the correlation, or detection signal on a group of parameters, x, y, z (which might represent target orientation, scale, contrast, etc.) is given as

$$C(x, y, z, \ldots) = f_x(x)\, f_y(y)\, f_z(z) \ldots \qquad (1)$$

For example, previous work on the M-50 tank using a third order matched filter, demonstrated that if $x = \theta$ (orientation of target) and y = linear scale of target, than the correlation signals varied as shown in Fig. 11. Now assume that we have constructed a bank of matched filters so that one memory address would have to

cover some specific set of target variations, for example, a $\pm\ \theta$ degree chage in orientation and a $\pm$ 10 percent change in scale. Further, assume that there will be other memory addresses to cover other specified ranges of target variables so that the entire memory bank will cover the entire range of target variations. Now since the target parameter values to be covered by any specific address can be anywhere in the stipulated ranges we will assume that the target parameters are independent random variables that are uniformly distributed over the stipulated ranges. Thus, we assume that the joint probability density function of the target parameters can be written as

$$P(x, y, z \ldots) = P_x(x)\ P_y(y)\ P_z(z) \ldots \tag{2}$$

and that, for example,

$$P_x(x) = \begin{cases} \dfrac{1}{2x_c} & , \quad -x_c < x < x_c \\ \\ 0 & , \quad \text{elsewhere} \end{cases} \tag{3}$$

where, for illustration, if $x = \theta$ (orientation angle) then x_c would be 8 degrees. Now if the variation of the correlation signal with the target parameters is a known function, than in theory we can compute the probability density function of the correlation signal C

$$P_C(c) = P(f_x\ f_y\ f_z \ldots) \tag{4}$$

and then finally the cumulative detection probability will be given by

$$P(C \leq C_o) = \int_{-\infty}^{C_o} P_C(c)\ dc \tag{5}$$

Equation (5) will enable us to determine the target detection performance of the single memory address since it yields the probability (P) that the correlation signal will be less than some given threshold C_o and it accounts for the variation of target parameters within the designed range to be covered by the single memory address. In other words given a threshold value C_o, $P(C \leq C_o)$ is the fraction of targets missed by the system. If we had a comparable plot of the fraction of false or clutter targets that exceeded the threshold C_o than we could combine $P(C \leq C_o)$ with these data to form a S/C detection tradeoff curve as shown in Fig. 12.

In order to proceed further we must make further assumptions concerning the variation of correlation signal with target variables. For the purpose of this report we will assume that the individual function given in Eq. (1) are each Gaussian, i.e., for example,

$$f_x(x) = e^{-(x/x_o)^2} \tag{6}$$

Note that if we assume that the memory address is designed to cover a change of a factor of 2 in the output correlation signal, then at the extremes of the target variable range, i.e., $x = \pm x_c$, we have

$$f_x(x_c) = 1/2 = e^{-(x_c/x_o)^2}$$

which requires that $(x_c/x_o) = \sqrt{\log 2}$. The next task is to determine the probability density function $P(C)$ given the assumed forms of f_x, and the probability density functions $P_x(x)$, $P_y(y)$, etc. To illustrate the analysis we will describe the results for the case when there are only two target parameters that can vary, i.e., $C = f_x(x)\, f_y(y)$. In this case we find (Ref. 3, p. 205)

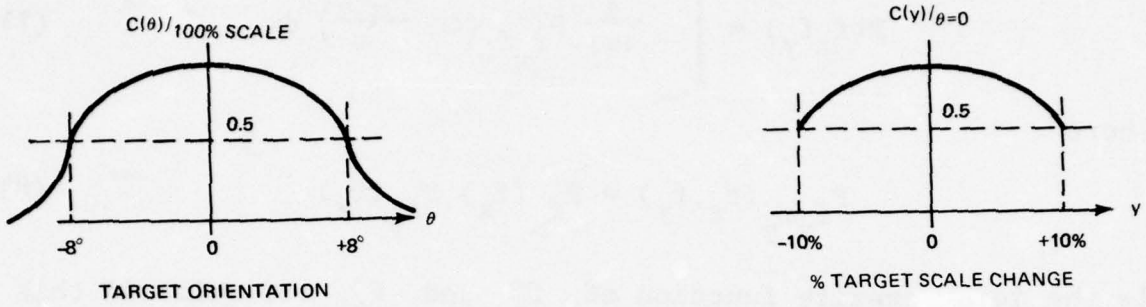

Fig. 11 Variation of *Correlation Signal* C with Target Parameter Changes Such as Orientation and Scale

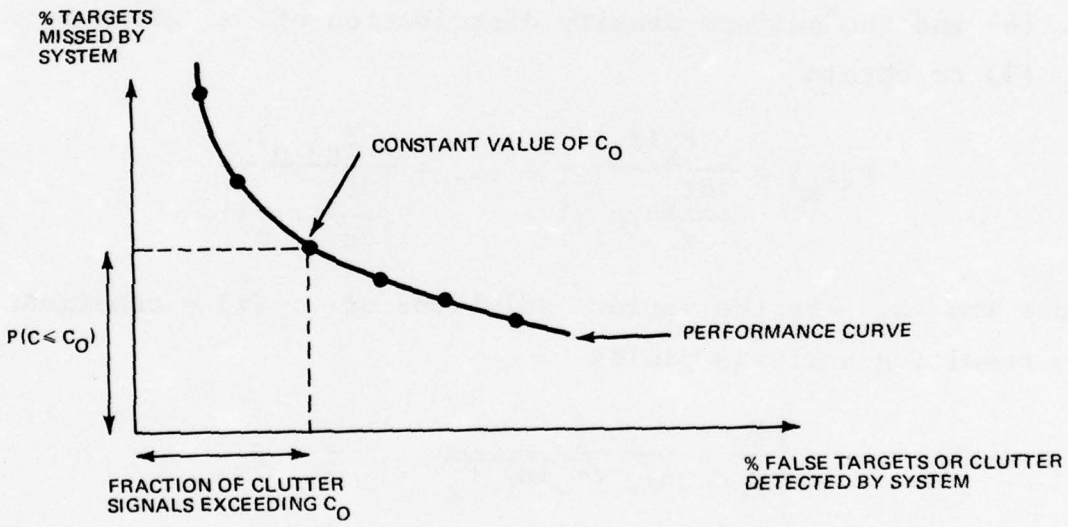

Fig. 12 Construction of Target/Clutter Detection Performance Characteristics

$$P(f_x f_y) = \int_{-\infty}^{\infty} \frac{1}{|\omega|} P_{f_x f_y}\left(\omega, \frac{f_x f_y}{\omega}\right) d\omega \tag{7}$$

where

$$P_{f_x f_y}(f_x, f_y) = P_{f_x}(f_x)\, P_{f_y}(f_y) \tag{8}$$

is the joint density function of $f_x^{\wedge}$ and $f_y^{\wedge}$ and which in this case are independent random variables that can be factored as shown. In order to find the individual probability density function, i.e., P_{f_x}, we utilize the assumed functional form of Eq. (6) and the uniform density distribution of x given by Eq. (3) to obtain

$$P(f_x) = \frac{P_x(x_1)}{\left|\frac{df_x}{dx}(\theta_1)\right|} + \ldots + \frac{P_x(x_u)}{\left|\frac{df_x}{dx}(x_u)\right|} \tag{9}$$

where the x_i are the various solutions of $f_x(x) = \text{constant}$. The resulting analysis yields

$$P(f_x) = \begin{cases} \frac{x_o}{x_c} \frac{1}{2f_x\sqrt{-\log f_x}}, & \frac{1}{2} < f_x < 1 \\ 0, & \text{elsewhere} \end{cases} \tag{10}$$

and in the present case where we assume that $f_x^{\wedge}$ drops to $1/2$ at $x = x_c$, we also have $x_c/x_o = \sqrt{\log 2}$. We may substitute this result into Eq. (7) to obtain

$$P(c) = P(f_x f_y) = \frac{1}{(2\sqrt{\log 2})^2} \int_{-\infty}^{\infty} \frac{1}{\omega} \frac{\ell(\omega)\ \ell\left(\frac{f_x f_y}{\omega}\right)}{\omega\sqrt{-\log \omega}\left(\frac{f_x f_y}{\omega}\right)\sqrt{-\log\left(\frac{f_x f_y}{\omega}\right)}}\, d\omega \tag{11}$$

where

$$\ell(z) = \begin{cases} 1 & , \quad \frac{1}{2} < z < 1 \\ 0 & , \quad \text{otherwise} \end{cases}$$

Finally, we compute the detection probability P as

$$P(C \leq C_o) = \int_{-\infty}^{C_o} P(C)dC = \frac{1}{4 \log 2} \int_{\frac{1}{2}}^{1} \frac{1}{\omega\sqrt{-\log \omega}}\, d\omega \int_{-\infty}^{C_o} \frac{\ell(C/\omega)}{C\sqrt{-\log(C/\omega)}}\, dC \tag{12}$$

After carrying out the indicated operations we obtain

$$P_2(C \leq C_o) = \begin{cases} 0 & , \quad C_o \leq \frac{1}{4} \\ 1 - \sqrt{\frac{-\log 2C_o}{\log 2}} + \frac{\log C_o}{\log 4} \sin^{-1}\left(\frac{\log 4C_o}{-\log C_o}\right) & , \quad \frac{1}{4} \leq C_o \leq \frac{1}{2} \\ 1 + \frac{\pi}{\log 16} \log C_o & , \quad \frac{1}{2} \leq C_o \leq 1 \\ 1 & , \quad 1 \leq C_o \end{cases} \tag{13}$$

where we have added the subscript P_2 to indicate that the result applies to the case where two target parameters can vary. Similar analysis, when only one target variable is considered, yields

$$P_1(C \leq C_o) = \begin{cases} 0 & C_o \leq \frac{1}{2} \\ 1 - \sqrt{\dfrac{-\log C_o}{\log 2}} & \frac{1}{2} \leq C_o \leq 1 \\ 1 & 1 \leq C_o \end{cases} \qquad (14)$$

The analysis for additional target variables becomes increasingly long; the result for three variables was only taken to the form

$$P_3(C \leq C_o) = \frac{1}{(2\sqrt{\log 2})^3} \int \frac{1}{\omega} A(\omega)\, B(\omega, C_o)\, d\omega \qquad (15)$$

where

$$A(\omega) = \begin{cases} 2 \sin^{-1}\left(\dfrac{\log 4\omega}{-\log \omega}\right) & \frac{1}{4} < \omega < \frac{1}{2} \\ \pi & \frac{1}{2} < \omega < 1 \\ 0 & \text{otherwise} \end{cases}$$

and

$$B(\omega, C_o) = \begin{cases} 2\left(\sqrt{\log 2} - \sqrt{\log(\omega/C_o)}\right) & C_o < \omega < 2C_o \\ 2\sqrt{\log 2} & \omega < C_o \\ 0 & \text{otherwise} \end{cases}$$

The results of the three analyses were computed numerically and are shown in Fig. 13.

We are now in a position to integrate this analysis with some of the typical clutter data found experimentally. Table 11 contains the results of a clutter assessment for two typical scenes wherein the threshold of $\hat{C} = 1$ or zero dB was established as

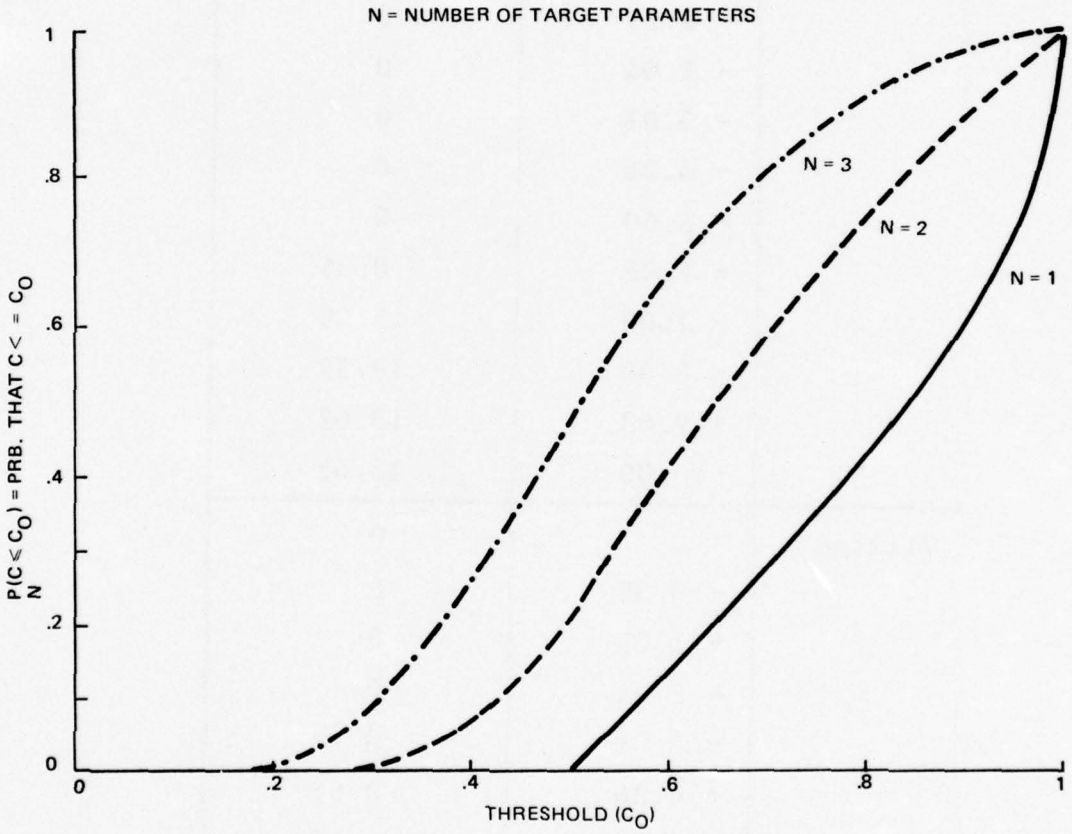

Fig. 13 Plots of Target Detection Probability as a function of Threshold Level and Number of Target Parameters that are varying statistically

TABLE 11 VARIATION OF PERCENT BACKGROUND CLUTTER ABOVE THRESHOLD FOR TWO BACKGROUND TERRAIN SCENES WITH A THIRD ORDER MATCHED FILTER OF AN M-60 TANK

Scene	Threshold	% Clutter Above Threshold
Woodland	$\hat{C}$	0
	- 0.58 dB	0
	- 1.25	0
	- 2.04	0
	- 3.01	0
	- 4.26	0
	- 5.00	0
	- 6.02	0.25
	- 7.00	5.49
	- 8.00	10.37
	- 9.03	13.02
	-10.00	16.42
Village	0	0
	- 0.58	0
	- 1.25	0
	- 2.04	0
	- 3.01	0
	- 4.26	0.67
	- 5.00	1.56
	- 6.02	4.74
	- 7.00	9.44
	- 8.00	15.93
	- 9.03	24.07
	-10.00	27.41

the peak autocorrelation signal for an M-60 tank. The information used to generate Table 11 was obtained by rerunning the tests on the woodland and village scenes; but in analyzing the data, additional threshold levels were used. There is considerable similarity between Tables 10 and 11, though they have only a few common threshold values. Now, as an illustration of the combination of these data with the previous analysis, we assume that a memory address is to be designed for a given number (N) of target parameter variations where each variation could individually cause a reduction of the target correlation signal to -3 dB. We then use Fig. 12 to merge the experimented data of Table 11 with the analytic data displayed in Fig. 13 to obtain the results shown in Fig. 14. These figures display the detection performance of both the woodland and village scenes as a function of the number of target parameters that the single memory address is designed to cover. For both types of background we had perfect performance when only one target parameter is allowed to vary, i.e., setting the threshold $C_o = 1/2$ or -3 dB yields $P(C \leq C_o) = 0$, i.e., zero percent missed targets, and simultaneously zero percent clutter detections. This was also the case for the woodland background when two target parameters were varied. The other cases are plotted in Fig. 14 in the range of percent errors below 10 percent.

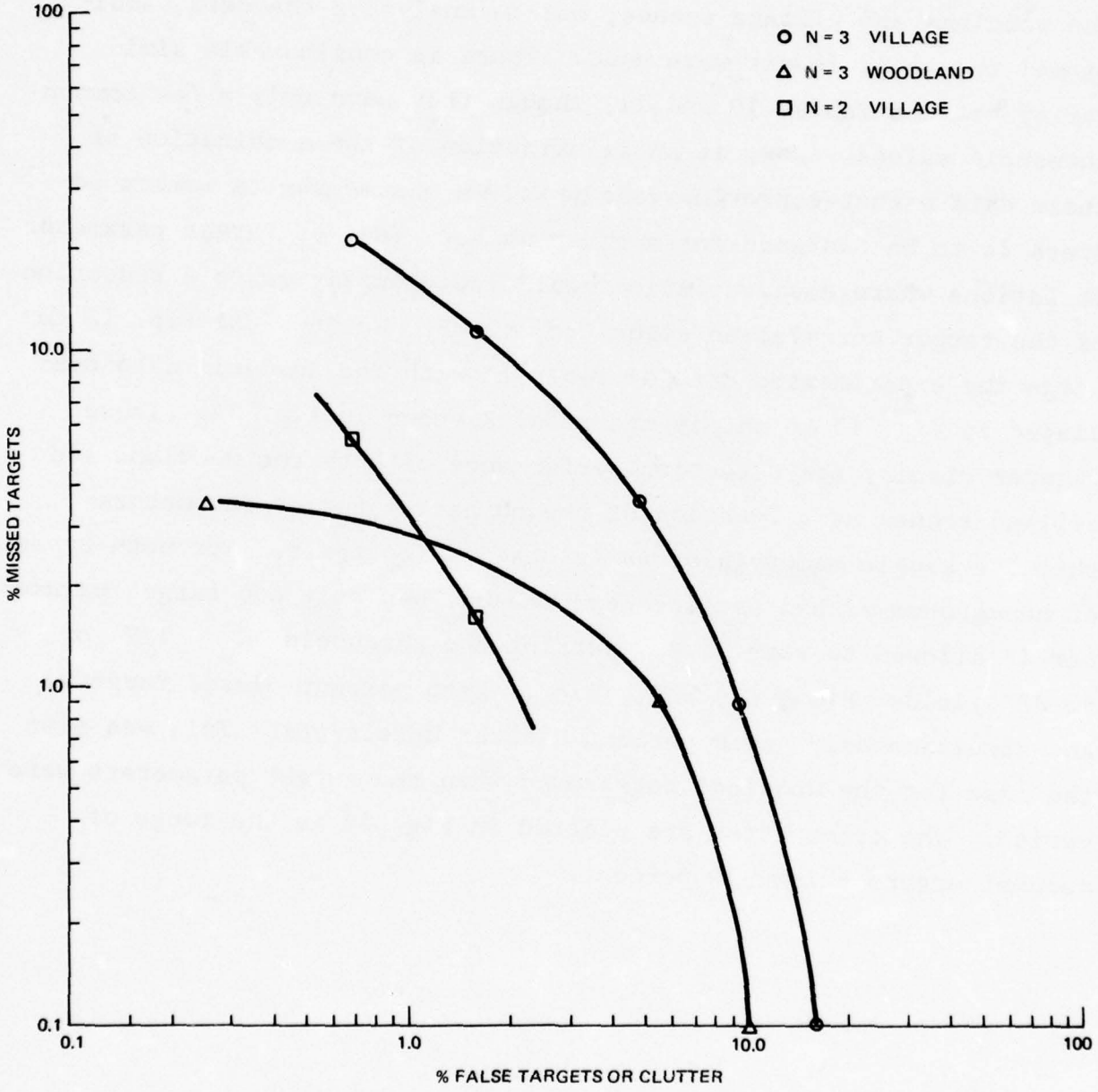

Fig. 14 Detection Performance of Single Address Third Order M-60 Matched Filter Covering Various Target Parameters (N = no. of parameters) and Two Typical Terrain Backgrounds

5. CONCLUSIONS

The results of this investigation were obtained by sampling in the correlation plane using one or more scan lines. The latter, related back to the input plane was approximately one-half of a standard television line. The effectiveness of this sampling in predicting the performance of an entire frame analysis was not qualified. In spite of the limited sampling in this program, it is believed that a number of conclusions can be drawn, and recommendations made, regarding further investigations on the OMFIC system. These are drawn from the work presented as well as from that in the appendix.

The OMFIC baseline correlator was able to handle a wide variety of complexity in terrain imagery and pick out the desired target, which in all cases was an M-60. Similar competing targets (e.g., T-62) did not present a problem for the high spatial frequency matched filters.

A statement was made in Ref. 4 that a target could be more easily picked out in the field rather than in town. This was based upon a study involving human examinations and assessments. The same statement might be made about the OMFIC system performance except that in the latter case, any reasonable threshold will always enable the target to be detected. Thus, while false alarms may result, the function of screening is accomplished.

It is also apparent that in our investigation — and in the case of a projected detector array — the smaller the probe the greater the S/C ratio the detection system "sees." This is another way of saying that true peak detection is desired in an OMFIC system.

Of considerable significance is the result that the false target presence (or what can be expressed in terms of the probability of detection) is very much a function of (a) the detection threshold level, and (b) the order of the matched filter employed in the correlator.

It is not surprising that film contrast plays a role in target detection. Autocorrelation signals increase with increasing target-background contrast and this result appears to reinforce the result presented in Ref. 1 where it was shown to be true regardless of whether the contrast was a negative or positive one.

Finally, in light of the results of Ref. 1 and the results of this study, it is concluded that the OMFIC technology is sufficiently advanced so that it has practical application to screening reconnaissance films.

6. REFERENCES

1. Leib, K. G., Bondurant, R. A., and Hsiao, S., "Optical Method Filtering Techniques for Automatic Interrogation of Aerial Reconnaissance Film," Final Report on Contract No. DAAG53-75-C-0199, September 1976.

2. Grumet, A. et al., Optical Matched Filter Image Correlator, Grumman Research Department Report RE-512, May 1975.

3. Papoulis, A., "Probability, Random Variables, and Stochastic Processes," McGraw-Hill Publishing Company, New York, 1965.

4. Ciavarelli, A., "Terrain Classification Study, USNWC, TP5766, May 1975.

APPENDIX

EFFECTS OF MATCHED FILTER ORDER PROBE SIZE AND FILM CONTRAST ON S/C RATIO

Various aspects of this sampling program were carried out but are considered more in support of, rather than a part of the main theme. These deal with the orders of matched filter, probe size, and contrast effects. Because of their ancillary importance, they are grouped together in this appendix.

SIGNAL/CLUTTER RATIO FOR VARIOUS ORDER MATCHED FILTERS

Tests were conducted using the Woodland, Roadside, and River/Island terrain scenes in which the S/C ratio was determined for each order of matched filter employed. As near as possible, the scan was made through the autocorrelation peak which was optimized for each of the matched filters prior to the scan.

The results are shown in Table A-1, where in addition to the S/C ratio, the relative signal strength is given. It is interesting to note that the relative signal strength is not too different from that obtained from the autocorrelation case. However, there is considerable variation in the S/C ratio where there is an indication that S/C ratio might be a function of the order of matched filter, a result one might intuitively anticipate.

Each of the curves obtained for the various orders of matched filters is shown in Figs. A-1, A-2, and A-3 for the Roadside scene. Note that there are large differences in vertical scale. It should be particularly noted that the maximum clutter does not necessarily occur at the same point in the scan line relative to the autocorrelation peak. The values for the matched filters are given in Table A-1.

TABLE A-1 S/C RATIO FOR CLUTTER LOCATED IN SAME POSITION FOR EACH MATCHED FILTER ORDER

Matched Filter Order	S/C Ratio for Same Clutter in Scan
0	1.00
1-3	5.01 dB
4	5.43
5	7.11
6	11.13

The same comments for Table A-2 notes apply. It should be noted that there is a significant difference in S/C ratio between that obtained from the peak clutter, and the same source of clutter. This in a limited way also supports the indication of a relationship between terrain character and matched filter order.

TABLE A-2 S/C RATIO AND RELATIVE SIGNALS FOR CENTERED LINE SCAN THROUGH M-60 TARGET IN RECONNAISSANCE SCENES

Matched Filter Order	Relative Signal Strength†			S/C Ratio (dB)		
	No. 1 Wooded Terrain	No. 2a Roadside Terrain	No. 3a River/Island Terrain	No. 1 Wooded Terrain	No. 2a Roadside Terrain	No. 3a River/Island Terrain
0	2.29‡	4.18‡	6.91‡	1.00	1.00	1.00
1-3	1.00	1.00	1.00	9.42	3.17	2.44
4	0.65	0.49	1.17	14.40	2.05	1.41
5	0.11	0.10	0.14	5.94	3.56	4.64
6	0.27	0.26	0.41	2.87	2.18	2.40

Note:

†Normalized to (1-3) order

‡Represents clutter, not M-60 correlation signal

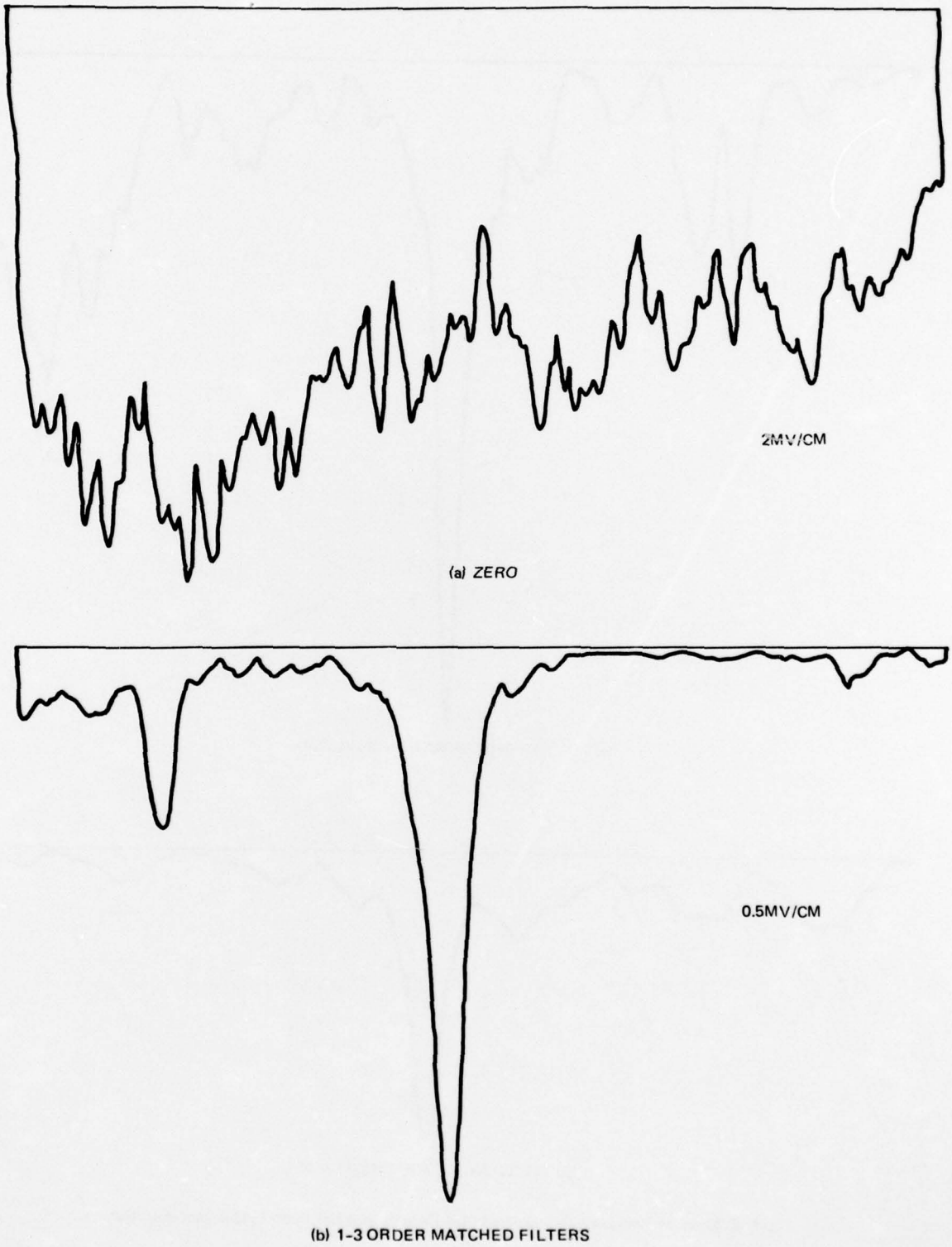

Fig. A-1 Scan of Roadside Scene Using (a) Zero and (b) 1-3 Order Matched Filters

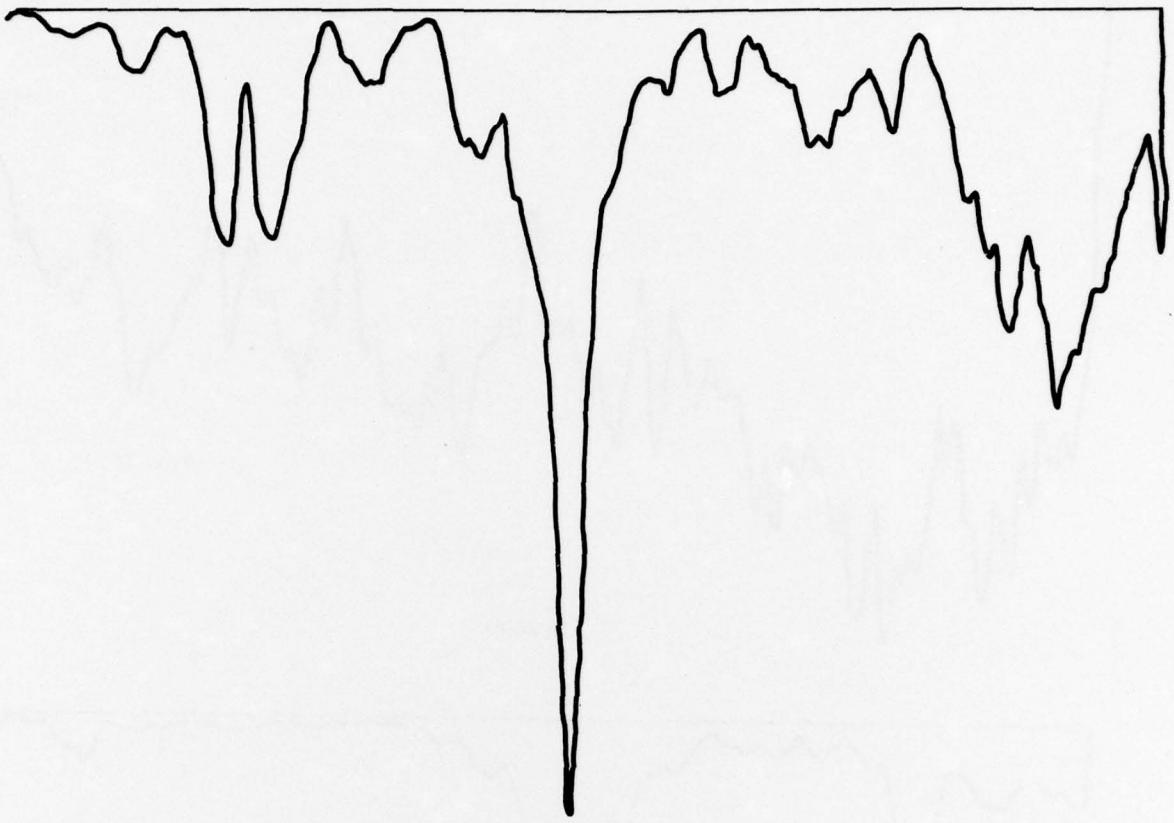

(a) FOURTH ORDER MATCHED FILTER

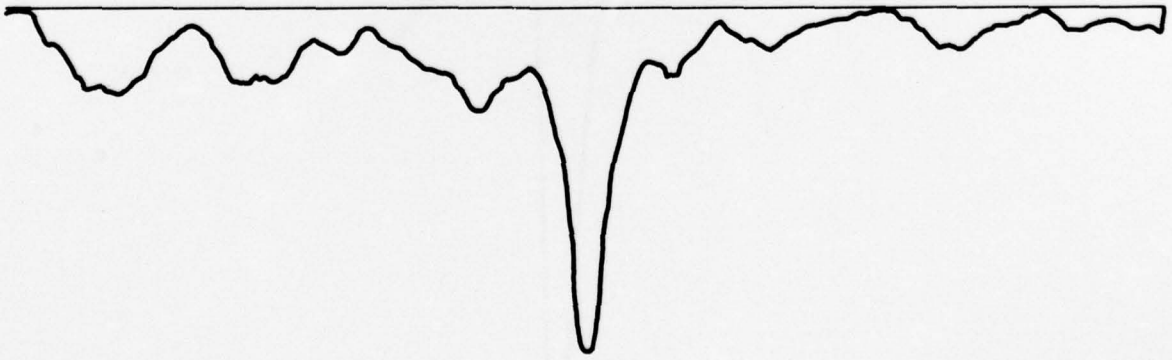

(b) FIFTH ORDER MATCHED FILTER

Fig. A-2 Scan of Roadside Scene Using (a) Fourth and (b) Fifth Order Matched Filters

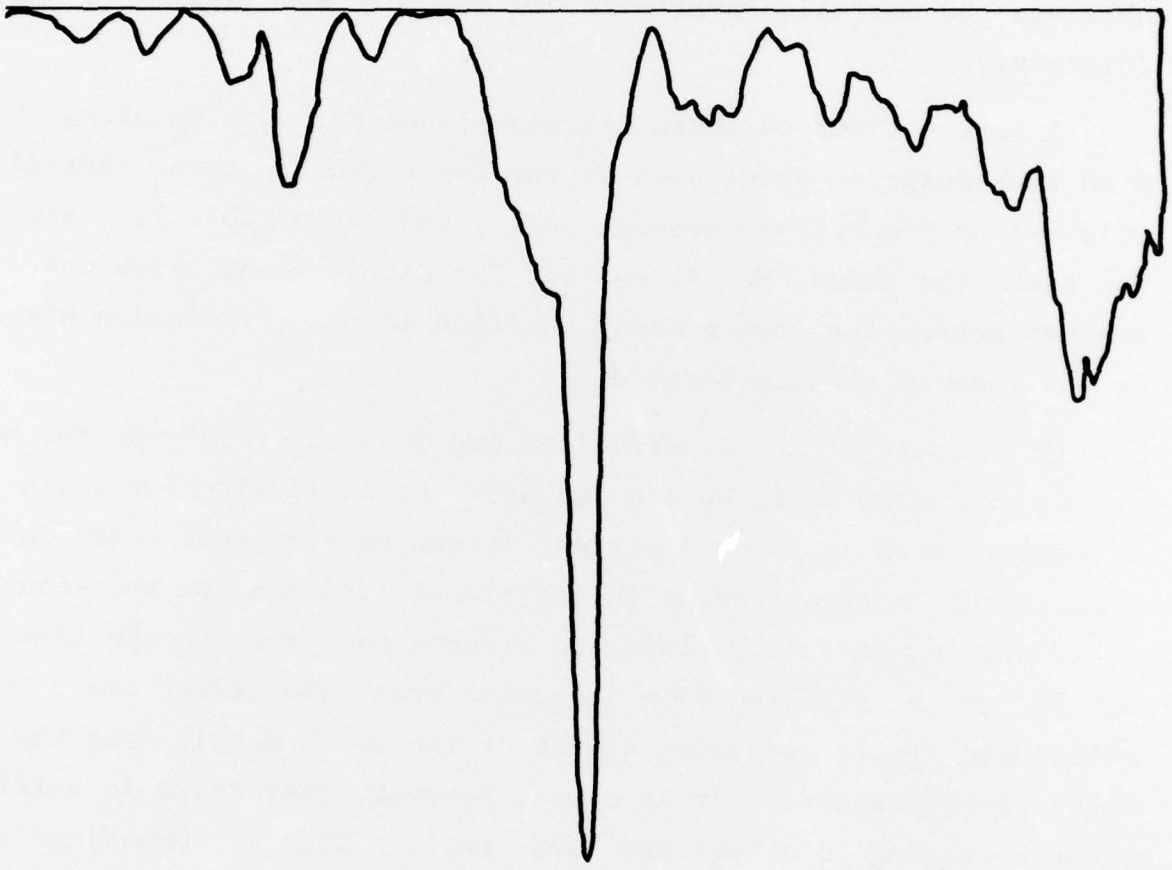

Fig. A-3 Scan of Roadside Scene Using Sixth Order Matched Filter

PROBE SIZE EFFECT

It was previously shown[†] that the autocorrelation peak for an M-60-like target 6 percent larger than that used in this investigation was quite sharp, enough so that correlation values measured with a 100 μm probe yielded peak values one-half those predicted by the simulation. In the current work, the smallest probe available was 50 μm. Also available was one that was 450 μm in size (diameter).

A test was run on three terrain scenes by scanning along the M-60 tank position using each of the two probes in turn. Actually only two of the terrain scenes, Nos. 1 and 3a in Table 2, contained the tank; the third, No. 4, was the Two Circle scene which was scanned across the same nominal position in the correlation plane as the tank is usually located.

The scans for the River/Island and Twon Circle scenes for both probes are shown in Figs. A-4 and A-5. Even allowing for small misregistration in probe location, it can be seen that there is considerable correspondence in positional location for the scans. It is also somewhat surprising to observe that even though there is an 81 to 1 difference in detection area, the larger probe shows relatively little averaging effect of the small detail over the small probe response. It is clear, however, that there is sufficient averaging to affect the S/C ratio. This is summarized in Table A-3. Here we can see that for both scenes containing a target, the S/C ratio is 33 and 82 percent greater, respectively, for the Woodland and River/Island scenes when the smaller probe is used.

[†] Ref. 1, pp. 60-61.

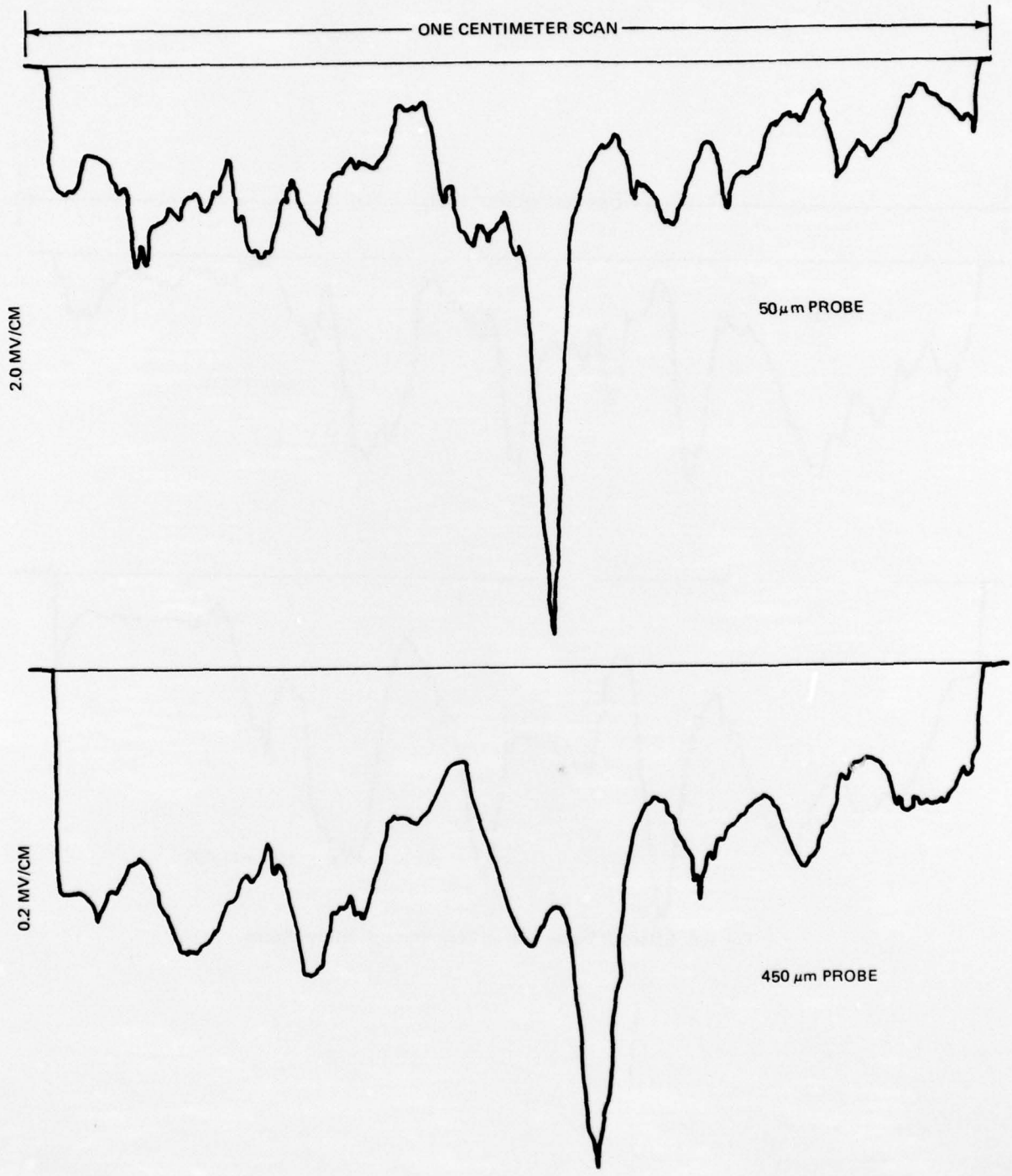

Fig. A-4 Effect of Probe Size on Scan Through M-60 Tank in River/Island Scene

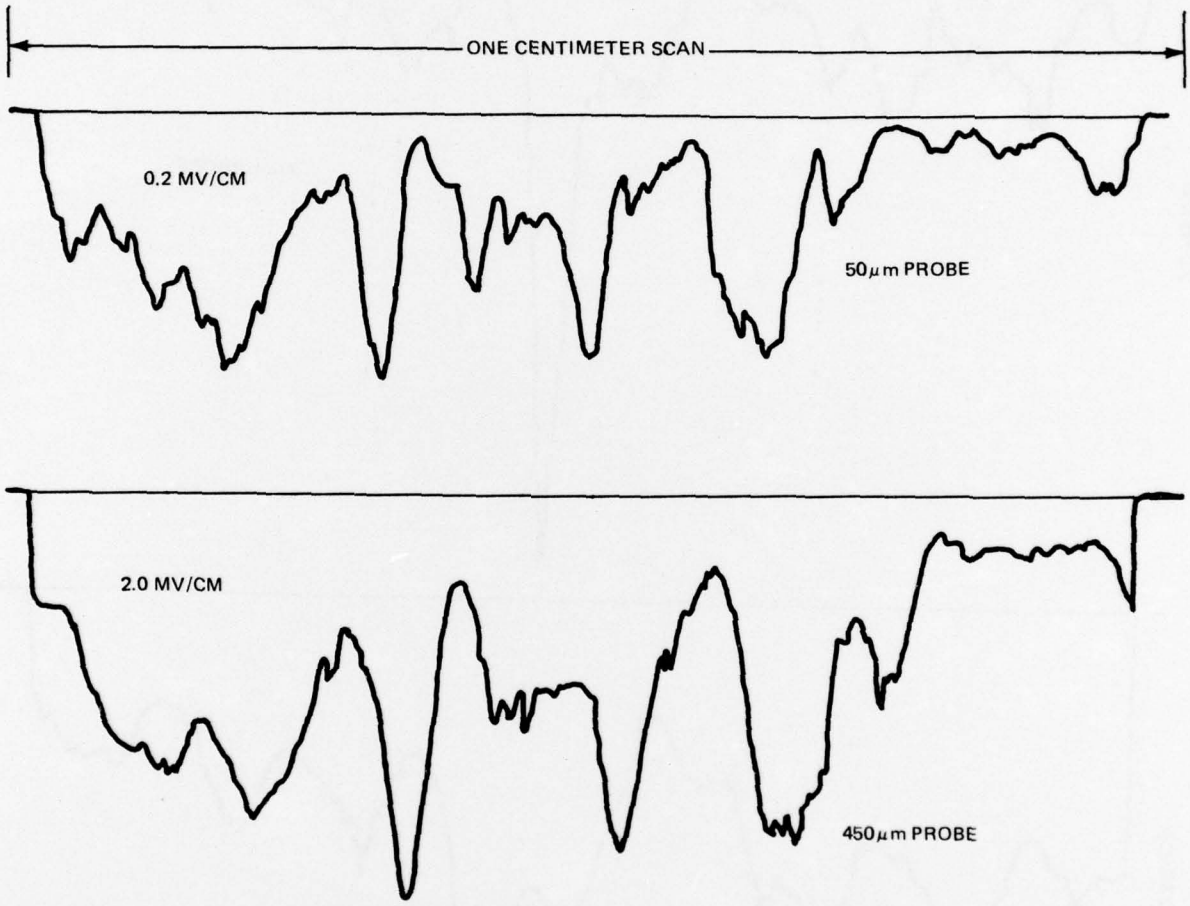

Fig. A-5 Effect of Probe Size on Scan Through Village Scene

TABLE A-3 EFFECTS OF DETECTOR PROBE SIZE UPON SIGNAL STRENGTH AND S/C RATIO FOR SIXTH ORDER MATCHED FILTER

Terrain	Relative Signal Level				S/C Ratio	
	M-60		Clutter			
	50	450	50	450	50	450
Woodland	0.20	0.96	0.04	0.34	3.76	2.82
River/Island	0.12	1.00	0.04	0.61	2.80	1.54
Village (No Targets)	-	-	0.04	0.68	-	-

Fortunately, information measured using the small probe assumes a lower peak value for the autocorrelation peak (because it also averages). At the same time, this probe more nearly responds to the peak clutter signals. This is based upon the observation that most, but not all clutter, tends to be broad.

In order to investigate the autocorrelation peak further, a scale set of different sized tanks was played through the third order matched filter. The autocorrelation peaks were measured both in magnitude and width. In accomplishing this, three or more scans were made through the peak region in order to assure that the peak value was most likely recorded. These measurements were made with the 50 μm probe and the scan was directed along the major tank axis.

The results are shown in Fig. A-6. The top plot is the half-width of the correlation peak at $x = y = 0$ versus M-60 tank size using a tank 0.94 x 1.88 mm on the object film as the 100 percent size. Due to the low magnitude of the signal at the extremes, the 53 and 160 percent scale size data points are considered to have less accuracy than the others. It is not entirely clear, but there appears to be a trend toward minimization at the extreme sizes as

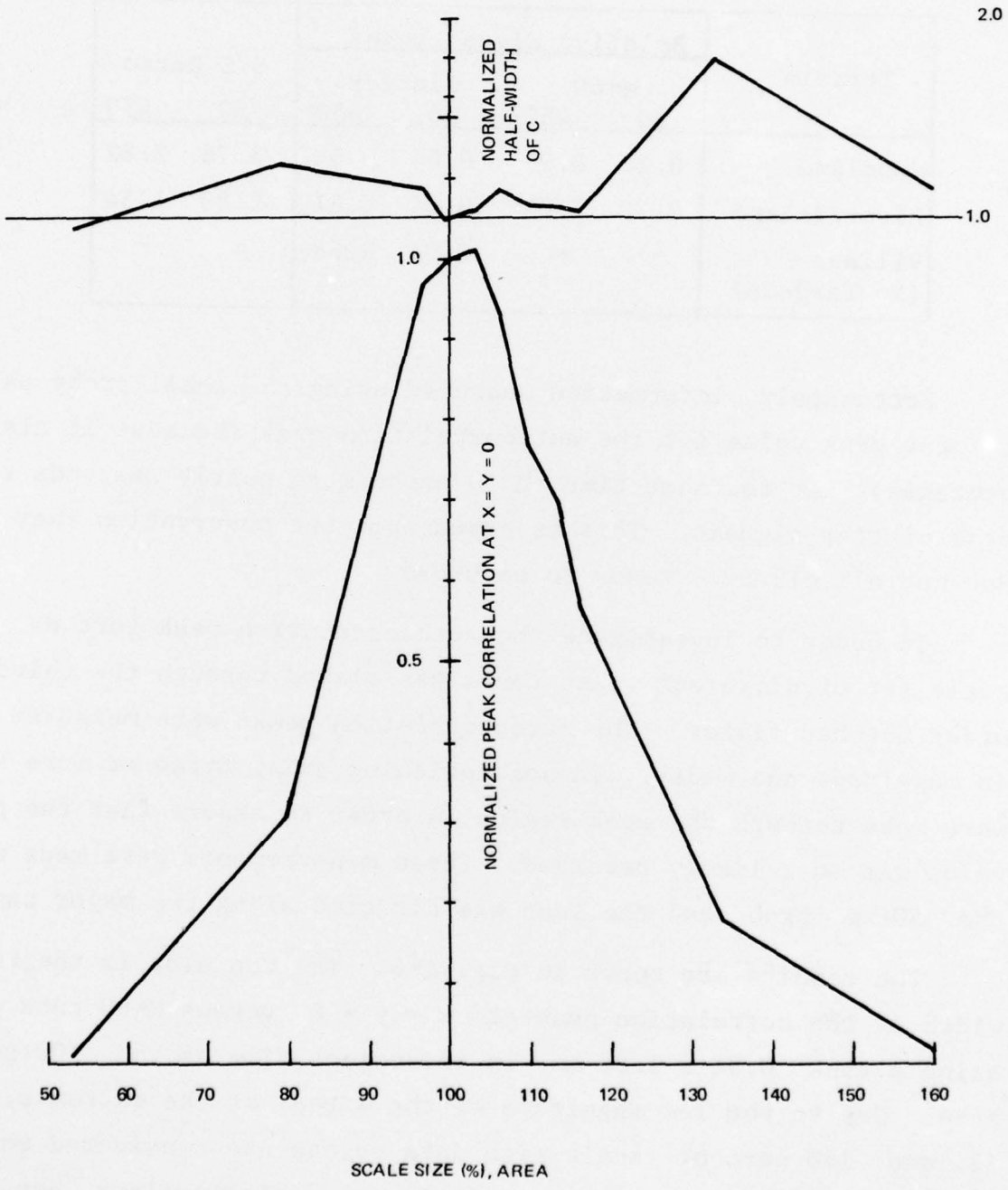

Fig. A-6 Normalized (a) Autocorrelation Peak width and (b) Scale Sensitivity For Third Order Filter

well as at the nominal 100 percent scale value. The latter was calculated to be about 180 μm, a value 8.9 percent of the tank length referenced back to the object plane.

It was not originally intended that any parametric sensitivities be determined in this investigation but a natural determination is the "spot size" of the correlation distribution. The results are shown in Fig. A-6b and are obtained from the same data used to obtain scale size sensitivity. The spot size referred to is the 3 dB width of the correlation. One of the objectives of the work in Ref. 1 was to derive the M-60 parametric sensitivities of a matched filter. Thus, it would be interesting to compare the present results with those. This is done in Table A-4.

TABLE A-4 COMPARISON OF SCALE SENSITIVITIES FOR DIFFERENT SIZE NORMALIZING TANKS

	% Below 100% Size	% Above 100% Size	% Total Interval
Ref. 1	-14.0	+21.7	35.7
Current Test	-16.9	+19.0	35.9

It can be seen that the results are practically identical even though the test were conducted a year apart. Some of the parameters involved in obtaining this information are as follows:

	Ref. 1	Current
100% Image	0.94 x 1.88 mm	1 x 2 mm
Image	Digital	Analog
Emulsion	Different Batches	
Scale Set	Digital	Digital
Orientation	Vertical	Horizontal
MF Optimum Point	Same	

The zero order of "DC" filter was also examined for size by scanning along the major tank axis. In this case, the peak values were not easily defined because of the presence of variations attributable to the presence of Newton's rings in the system, and the absence of uniformity in the matched filter and similar small, but accuracy disturbing anomalies. With these limitations the scale set of images were played through the filter and the data examined. In contrast to the results above, the half width of the DC spot size in the correlation plane peaks up at the 100 percent scale size and at the ends, and then dips down between these points. The average spot size for all readings was 1.03 mm with the value for the 100 percent image (0.97 x 1.94 mm) being 1.09 mm. If we were to compute the percentage that the spot size is of the true size along the long dimension of the tank, the direction of scan, we find it follows the spot size distribution by peaking up at the 100 percent and, at the 50 and 150 percent sizes. Except for the 50 percent size case (0.82), all other values are close to 50 percent with the 100 percent size image being 56 percent of its size in the film.

EFFECT OF CONTRAST ON S/C RATIO

One of the results of the simulations conducted during the program described in Ref. 1 was that the (autocorrelation) S/C ratio was greatest for the largest target background contrast ratio C_R and, that this S/C ratio decreased to zero when $C_R = 0$. Further, a curve of C_R versus S/C shows the relationship is nearly symmetrical about $C_R = 0$ for positive or negative targets. The sign refers to the cases where the target signal intensity is greater or less than the associated background. Note that positive or negative targets yield negative or positive contrast ratios.

These results are described on Pages 54-63 of that reference. In the above the following definitions were used:

$$C_R = \frac{I_{AP} - I_{TGT}}{I_{AP} + I_{TGT}}$$

$$S/C = \frac{\text{Peak autocorrelation signal}}{\text{Peak background in correlation plane}}$$

The results referred to above were obtained using uniform density, square targets against uniform density circular background apertures. However, the results seem to be a reasonable prediction of what to expect for military targets whose contrast with backgrounds can vary widely.

During the fabrication of the terrain test film strip three additional images were prepared of the Woodland scene in which the contrast was varied. They were played through the third order matched filter, and scans made through the autocorrelation peak along the tank axis. The results are shown in Fig. A-7. Measurements of the signal and clutter were made and are given in Table A-5 along with some of the scene image parameters. The relative signal strength is taken with respect to the autocorrelation signal shown in Fig. A-8.

TABLE A-5 TEST RESULTS OF SCENES IN WHICH CONTRAST IS DIFFERENT

Image	Contrast Ratio C_R †	Average Optical Density	Relative Signal Strength ‡	S/C Ratio	
				Same Clutter	Peak Clutter
17a	0.89	0.66	0.22	8.58 dB	8.58 dB
17b	0.87	0.24	0.075	6.67	4.59
17c	0.55	0.09	0.043	3.20	0.51

† $C_R = (I_x - I_N)/(I_x + I_N)$ where $I_{x,N}$ represent maximum, minimum intensities of signal when original film is reimaged and scanned.

‡ Relative to autocorrelation

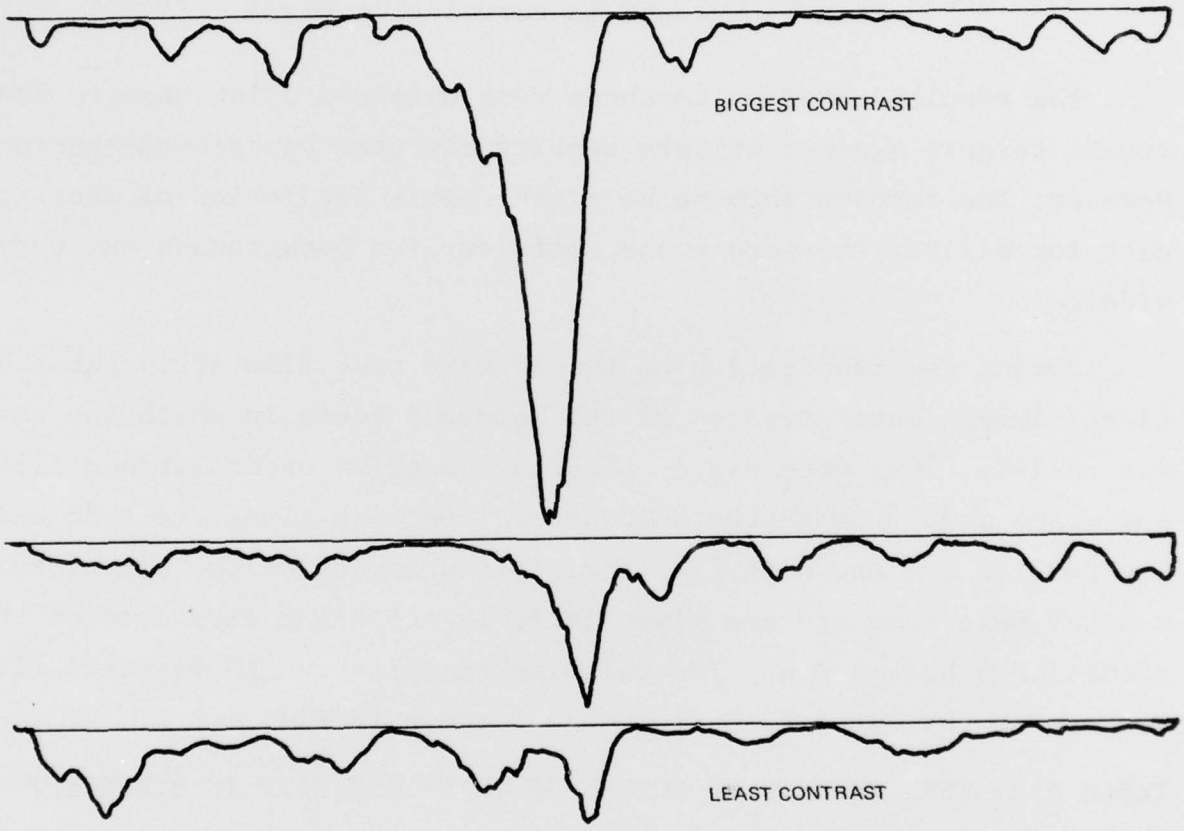

Fig. A-7 Scans Through Target in Woodland Scenes of Different Contrast (to same vertical scale)

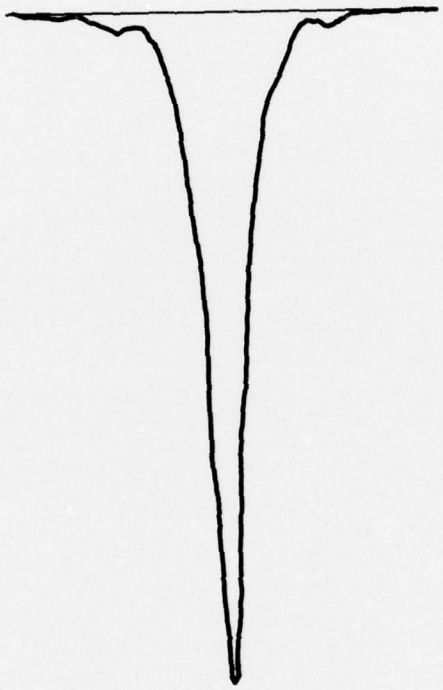

Fig. A-8 M-60 Autocorrelation Peak